Reporter Assay for *srebp-1c* Promoter Activity. The genomic DNA fragment encoding the *srebp-1c* promoter region (located from residues −410 to +24) was amplified from a mouse genome. The fragment was introduced into the KpnI and HindIII sites of pGL3-Basic (Promega, Madison, WI), and it was designated as pGL3-srebp-1cPro. The plasmids encoding RXRα and LXRα were transfected into MEFs together with pGL3-srebp-1cPro and a control plasmid encoding *Renilla* luciferase (Promega). The total DNA for transfection was normalized by the addition of empty plasmids. Cells were harvested at 24 h posttransfection. The ligand of RXRα, 9-*cis*-retinoic acid (Sigma), and that of LXRα, 22(*R*)-hydroxylcholesterol (Sigma) were added at a final concentration of 5 μM each to the culture medium of 293T cells transfected with pGL3-srebp-1cPro together with expression plasmids encoding RXRα, LXRα, and HCV core protein at 24 h posttransfection. Cells were harvested 24 h after treatment. Luciferase activity was measured by using the dual-luciferase reporter assay system (Promega). Firefly luciferase activity was standardized with that of *Renilla* luciferase, and the results are expressed as the fold increase in relative luciferase units.

Electrophoresis Mobility Shift Assay (EMSA). EMSA was carried out by using a LightShift Chemiluminescent EMSA kit (Pierce) according to the manufacturer's protocol. Nuclear extract of the cell lines and liver tissue was prepared with an NE-PER nuclear and cytoplasmic extraction reagent kit (Pierce). Briefly, double-stranded oligonucleotides for EMSA were prepared by annealing both strands of each LXRE of the *srebp-1c* promoter (5′-GGACGCCCGCTAGTAACCCCGGC-3′) (16). Both strands were labeled at the 5′ ends with biotin. The annealed probe was incubated for 20 min on ice with nuclear extract (3 μg of protein) in a reaction buffer containing 10 mM Tris·HCl (pH 7.5), 50 mM KCl, 1 mM DTT, 0.05 μg/μl poly(dI-dC), 2.5% glycerol, 0.05% Nonidet P-40, and 0.1 nM labeled probe, with or without 1 mM nonlabeled probe. The resulting mixture was subjected to PAGE (5% gel) at 120 V for 30 min in 0.5× TBE. The DNA–protein complex was transferred to a Hybond N+ membrane (Amersham, Piscataway, NJ), incubated with horseradish peroxidase-conjugated streptavidin, and visualized by using an LAS3000 imaging system.

Statistical Analysis. The results are expressed as the mean ± SD. The significance of differences in the means was determined by Student's *t* test.

1. Wasley A, Alter MJ (2000) *Semin Liver Dis* 20:1–16.
2. Bach N, Thung SN, Schaffner F (1992) *Hepatology* 15:572–577.
3. Lefkowitch JH, Schiff ER, Davis GL, Perrillo RP, Lindsay K, Bodenheimer HC, Jr., Balart LA, Ortego TJ, Payne J, Dienstag JL, *et al.* (1993) *Gastroenterology* 104:595–603.
4. Barba G, Harper F, Harada T, Kohara M, Goulinet S, Matsuura Y, Eder G, Schaff Z, Chapman MJ, Miyamura T, Brechot C (1997) *Proc Natl Acad Sci USA* 94:1200–1205.
5. Hope RG, McLauchlan J (2000) *J Gen Virol* 81:1913–1925.
6. Moriya K, Fujie H, Shintani Y, Yotsuyanagi H, Tsutsumi T, Ishibashi K, Matsuura Y, Kimura S, Miyamura T, Koike K (1998) *Nat Med* 4:1065–1067.
7. Kapadia SB, Chisari FV (2005) *Proc Natl Acad Sci USA* 102:2561–2566.
8. Su AI, Pezacki JP, Wodicka L, Brideau AD, Supekova L, Thimme R, Wieland S, Bukh J, Purcell RH, Schultz PG, Chisari FV (2002) *Proc Natl Acad Sci USA* 99:15669–15674.
9. Wang C, Gale M, Jr, Keller BC, Huang H, Brown MS, Goldstein JL, Ye J (2005) *Mol Cell* 18:425–434.
10. Horton JD, Shimomura I, Brown MS, Hammer RE, Goldstein JL, Shimano H (1998) *J Clin Invest* 101:2331–2339.
11. Pai JT, Guryev O, Brown MS, Goldstein JL (1998) *J Biol Chem* 273:26138–26148.
12. Shimano H, Horton JD, Hammer RE, Shimomura I, Brown MS, Goldstein JL (1996) *J Clin Invest* 98:1575–1584.
13. Shimano H, Horton JD, Shimomura I, Hammer RE, Brown MS, Goldstein JL (1997) *J Clin Invest* 99:846–854.
14. Shimano H, Shimomura I, Hammer RE, Herz J, Goldstein JL, Brown MS, Horton JD (1997) *J Clin Invest* 100:2115–2124.
15. Repa JJ, Liang G, Ou J, Bashmakov Y, Lobaccaro JM, Shimomura I, Shan B, Brown MS, Goldstein JL, Mangelsdorf DJ (2000) *Genes Dev* 14:2819–2830.
16. Yoshikawa T, Shimano H, Amemiya-Kudo M, Yahagi N, Hasty AH, Matsuzaka T, Okazaki H, Tamura Y, Iizuka Y, Ohashi K, *et al.* (2001) *Mol Cell Biol* 21:2991–3000.
17. Tsutsumi T, Suzuki T, Shimoike T, Suzuki R, Moriya K, Shintani Y, Fujie H, Matsuura Y, Koike K, Miyamura T (2002) *Hepatology* 35:937–946.
18. Moriishi K, Okabayashi T, Nakai K, Moriya K, Koike K, Murata S, Chiba T, Tanaka K, Suzuki R, Suzuki T, *et al.* (2003) *J Virol* 77:10237–10249.
19. Masson P, Andersson O, Petersen UM, Young P (2001) *J Biol Chem* 276:1383–1390.
20. Li J, Rechsteiner M (2001) *Biochimie* 83:373–383.
21. Li X, Lonard D, Jung SY, Malovannaya A, Feng Q, Qin J, Tsai SY, Tsai M, O'Malley BW (2006) *Cell* 124:381–392.
22. Murata S, Kawahara H, Tohma S, Yamamoto K, Kasahara M, Nabeshima Y, Tanaka K, Chiba T (1999) *J Biol Chem* 274:38211–38215.
23. Falcon V, Acosta-Rivero N, Chinea G, Gavilondo J, de la Rosa MC, Menendez I, Duenas-Carrera S, Vina A, Garcia W, Gra B, *et al.* (2003) *Biochem Biophys Res Commun* 305:1085–1090.
24. Suzuki R, Sakamoto S, Tsutsumi T, Rikimaru A, Tanaka K, Shimoike T, Moriishi K, Iwasaki T, Mizumoto K, Matsuura Y, *et al.* (2005) *J Virol* 79:1271–1281.
25. Moriya K, Yotsuyanagi H, Shintani Y, Fujie H, Ishibashi K, Matsuura Y, Miyamura T, Koike K (1997) *J Gen Virol* 78:1527–1531.
26. Yasui K, Wakita T, Tsukiyama-Kohara K, Funahashi SI, Ichikawa M, Kajita T, Moradpour D, Wands JR, Kohara M (1998) *J Virol* 72:6048–6055.
27. Suzuki R, Tamura K, Li J, Ishii K, Matsuura Y, Miyamura T, Suzuki T (2001) *Virology* 280:301–309.
28. Minami Y, Kawasaki H, Minami M, Tanahashi N, Tanaka K, Yahara I (2000) *J Biol Chem* 275:9055–9061.
29. Watashi K, Hijikata M, Tagawa A, Doi T, Marusawa H, Shimotohno K (2003) *Mol Cell Biol* 23:7498–7509.
30. Machida K, Cheng KT, Lai CK, Jeng KS, Sung VM, Lai MM (2006) *J Virol* 80:7199–7207.
31. Nystrom T (2005) *EMBO J* 24:1311–1317.
32. Bromberg JF, Wrzeszczynska MH, Devgan G, Zhao Y, Pestell RG, Albanese C, Darnell JE, Jr (1999) *Cell* 98:295–303.
33. Carballo M, Conde M, El Bekay R, Martin-Nieto J, Camacho MJ, Monteseirin J, Conde J, Bedoya FJ, Sobrino F (1999) *J Biol Chem* 274:17580–17586.
34. Aizaki H, Aoki Y, Harada T, Ishii K, Suzuki T, Nagamori S, Toda G, Matsuura Y, Miyamura T (1998) *Hepatology* 27:621–627.
35. Niwa H, Yamamura K, Miyazaki J (1991) *Gene* 108:193–199.
36. Huang DC, Cory S, Strasser A (1997) *Oncogene* 14:405–414.
37. Aoyagi K, Ohue C, Iida K, Kimura T, Tanaka E, Kiyosawa K, Yagi S (1999) *J Clin Microbiol* 37:1802–1808.

Involvement of the PA28γ-Dependent Pathway in Insulin Resistance Induced by Hepatitis C Virus Core Protein[∇]

Hironobu Miyamoto,[1] Kohji Moriishi,[1] Kyoji Moriya,[2] Shigeo Murata,[3] Keiji Tanaka,[3] Tetsuro Suzuki,[4] Tatsuo Miyamura,[4] Kazuhiko Koike,[2] and Yoshiharu Matsuura[1]*

Department of Molecular Virology, Research Institute for Microbial Diseases, Osaka University, Osaka,[1] Department of Internal Medicine, Graduate School of Medicine, University of Tokyo, Tokyo,[2] Department of Molecular Oncology, Tokyo Metropolitan Institute of Medical Science, Tokyo,[3] and Department of Virology II, National Institute of Infectious Diseases, Tokyo,[4] Japan

The hepatitis C virus (HCV) core protein is a component of nucleocapsids and a pathogenic factor for hepatitis C. Several epidemiological and experimental studies have suggested that HCV infection is associated with insulin resistance, leading to type 2 diabetes. We have previously reported that HCV core gene-transgenic (PA28γ$^{+/+}$CoreTg) mice develop marked insulin resistance and that the HCV core protein is degraded in the nucleus through a PA28γ-dependent pathway. In this study, we examined whether PA28γ is required for HCV core-induced insulin resistance in vivo. HCV core gene-transgenic mice lacking the PA28γ gene (PA28γ$^{-/-}$CoreTg) were prepared by mating of PA28γ$^{+/+}$CoreTg with PA28γ-knockout mice. Although there was no significant difference in the glucose tolerance test results among the mice, the insulin sensitivity in PA28γ$^{-/-}$CoreTg mice was recovered to a normal level in the insulin tolerance test. Tyrosine phosphorylation of insulin receptor substrate 1 (IRS1), production of IRS2, and phosphorylation of Akt were suppressed in the livers of PA28γ$^{+/+}$CoreTg mice in response to insulin stimulation, whereas they were restored in the livers of PA28γ$^{-/-}$CoreTg mice. Furthermore, activation of the tumor necrosis factor alpha promoter in human liver cell lines or mice by the HCV core protein was suppressed by the knockdown or knockout of the PA28γ gene. These results suggest that the HCV core protein suppresses insulin signaling through a PA28γ-dependent pathway.

Hepatitis C virus (HCV) is the causative agent in most cases of acute and chronic non-A, non-B hepatitis (15). Over one-half of patients with the acute infection evolve into a persistent carrier state (24). Chronic infection with HCV frequently induces hepatic steatosis, cirrhosis, and eventually hepatocellular carcinoma (22) and is known to be associated with diseases of extrahepatic organs, including an essential mixed cryoglobulinemia, porphyria cutanea tarda, membranoproliferative glomerulonephritis, and type 2 diabetes (13).

HCV is classified into the genus *Hepacivirus* of the family *Flaviviridae* and possesses a viral genome consisting of a single positive-strand RNA with a nucleotide length of about 9.5 kb. This viral genome encodes a single polyprotein composed of approximately 3,000 amino acids (9). The polyprotein is post-translationally cleaved by host cellular peptidases and viral proteases, resulting in 10 viral proteins (6, 10, 12). The HCV core protein is known to interact with viral-sense RNA of HCV to form the viral nucleocapsid (44). The HCV core protein is cleaved off at residue 191 by the host signal peptidase to release it from the E1 envelope protein and then by the host signal peptide peptidase at around amino acid residues 177 to 179 within the C-terminal transmembrane region (30, 39, 40). The mature core protein is retained mainly on the endoplasmic reticulum, although a portion moves to the nucleus and mitochondria (11, 51).

Recent epidemiological studies have indicated that type 2 diabetes is an HCV-associated disease (7, 29). However, it remains unclear how insulin resistance is induced in patients chronically infected with HCV, since there is no suitable model for investigating HCV pathogenesis. Type 2 diabetes is a complex, multisystemic disease with pathophysiology that includes a high level of hepatic glucose production and insulin resistance, which contribute to the development of hyperglycemia (8, 18). Although the precise mechanism by which these factors contribute to the induction of insulin resistance is difficult to understand, a high level of insulin production by pancreatic β cells under a state of insulin resistance is common in the development of type 2 diabetes. The hyperinsulinemia in the fasting state that is observed relatively early in type 2 diabetes is considered to be a secondary response that compensates for the insulin resistance (8, 18).

The HCV core protein is also known as a pathogenic factor that induces steatosis and hepatocellular carcinoma in mice (33, 35). Previously, we reported that insulin resistance occurs in HCV core gene-transgenic mice due at least partly to an increase in tumor necrosis factor alpha (TNF-α) secretion (47) and that the HCV core protein is degraded through a PA28γ/ REGγ (11S regulator)-dependent pathway in the nucleus (32). It is well known that PA28γ enhances latent proteasome activity, although the biological significance of PA28γ is largely unknown, with the exception that PA28γ is known to regulate steroid receptor coactivator 3 (28). Although several reports suggested that the degradation of insulin receptor substrate (IRS) proteins by a ubiquitin-dependent proteasome activity contributes to insulin resistance (43, 50), the involvement of the HCV core protein in cooperation with PA28γ in the stability of IRS proteins and in the development of insulin resis-

tance is not known. In this study, we examined the involvement of PA28γ in the induction of insulin resistance by the HCV core protein in vivo.

MATERIALS AND METHODS

Preparation of PA28γ-knockout HCV core gene-transgenic mice. C57BL/6 mice carrying the gene encoding HCV core protein genotype 1b (PA28$\gamma^{+/+}$ CoreTg) line C49 and PA28$\gamma^{-/-}$ mice have been described previously (35, 36). These two genotypes were crossbred to create PA28$\gamma^{+/-}$CoreTg mice. PA28$\gamma^{+/-}$CoreTg mice were bred to generate PA28$\gamma^{-/-}$CoreTg mice (35, 36). The HCV core gene and the target sequence to knock out the PA28γ gene were identified by PCR. The mice were given ordinary feed (CRF-1; Charles River Laboratories, Yokohama, Japan) and were maintained under specific-pathogen-free conditions.

Glucose tolerance test. The mice were fasted for more than 16 h before glucose administration. D-Glucose (1 g/kg body weight) was intraperitoneally administered to the mice. Blood samples were taken from the orbital sinus at the indicated time points. The plasma glucose concentration was measured by means of a MEDI-SAFE Mini blood glucose monitor (TERUMO, Tokyo, Japan). The serum insulin level was determined by a Mercodia (Uppsala, Sweden) ultrasensitive mouse insulin enzyme-linked immunosorbent assay (ELISA).

Insulin tolerance test. The mice were fed freely and then fasted during the study period. Human insulin (2 U/kg body weight) (Humulin; Eli Lilly, Indianapolis, IN) was intraperitoneally administered to the mice. The plasma glucose concentration was measured at the indicated time and was normalized based on the glucose concentration at the time just before insulin administration.

Histological analysis of pancreatic islets. Pancreas tissues were fixed with paraformaldehyde, embedded in paraffin, sectioned, and stained with hematoxylin and eosin. The relative islet area and islet number were determined with Image-Pro PLUS image analyzing software (NIPPON ROPER, Tokyo, Japan).

Estimation of tumor necrosis factor alpha and HCV core protein. Mouse TNF-α was measured by using a mouse TNF-α ELISA kit (Pierce, Rockford, IL) and normalized based on the amount of total protein in each sample. The protein concentration was estimated by using a BCA protein assay kit (Pierce). The amount of HCV core protein in the liver tissues was determined by using an ELISA system as described previously (4).

In vivo insulin stimulation and immunoblot analysis. Mice were fasted for more than 16 h before insulin stimulation and then anesthetized with ketamine and xylazine. Five units of insulin were injected into the mice via the interior vena cava. Livers of the mice were collected 5 min after the insulin injection and frozen in liquid nitrogen. Immunoblot analyses of the HCV core protein, PA28γ, and each of the insulin-signaling molecules were carried out with the liver tissue homogenates prepared in the homogenizing buffer containing 25 mM Tris-HCl (pH 7.4), 10 mM Na$_3$VO$_4$, 100 mM NaF, 50 mM Na$_4$P$_2$O$_7$, 10 mM EGTA, 10 mM EDTA, 2 mM phenylmethylsulfonyl fluoride, and 1% Nonidet P40 supplemented with Complete Protease Inhibitor Cocktail (Roche Diagnostics, Mannheim, Germany) (53). Tissue lysates were subjected to sodium dodecyl sulfate-2% to 15% gradient polyacrylamide gel electrophoresis (PAG Mini DAIICHI 2/15 13W; Daiichi Diagnostics, Tokyo, Japan) and electrotransferred onto polyvinylidene difluoride membranes (Immobilon-P; Millipore, Bedford, MA). The protein transferred onto the membrane was reacted with rabbit anti-HCV core (32), rabbit anti-Akt (Cell Signaling, Danvers, MA), rabbit anti-phospho-Ser473-Akt (Cell Signaling), rabbit anti-IRS1 (Upstate, Lake Placid, NY), rabbit anti-phospho-Tyr608 mouse insulin receptor substrate 1 (Sigma, St. Louis, MO), or rabbit anti-IRS2 (Upstate) polyclonal antibody and then incubated with horseradish peroxidase-conjugated anti-rabbit antibody. Blotted protein was visualized using Super Signal Femto (Pierce) and an LAS3000 imaging system (Fuji Photo Film, Tokyo, Japan).

Quantitative reverse transcription-PCR (RT-PCR). Total RNA was isolated from mouse liver using an RNeasy kit (QIAGEN, Valencia, CA). The RNA preparation was treated with a TURBO DNA-free kit (Ambion, Austin, TX) to remove DNA contamination in the samples. The first-strand cDNAs were synthesized by a first-strand cDNA synthesis kit (Amersham Biosciences, Franklin Lakes, NJ). The targeted cDNA was estimated by using Platinum SYBR Green qPCR Super Mix UDC (Invitrogen, Carlsbad, CA) according to the manufacturer's protocol. The fluorescent signal was measured by using an ABI Prism 7000 (Applied Biosystems, Foster City, CA). The genes encoding mouse TNF-α, IRS1, IRS2, and hypoxanthine phosphoribosyl transferase were amplified with the following primer pairs: 5'-GGTACAACCCATCGGCTGGCA-3' (forward) and 5'-GCGACGTGGAACTGGCAGAAG-3' (reverse) for TNF-α, 5'-ATAG
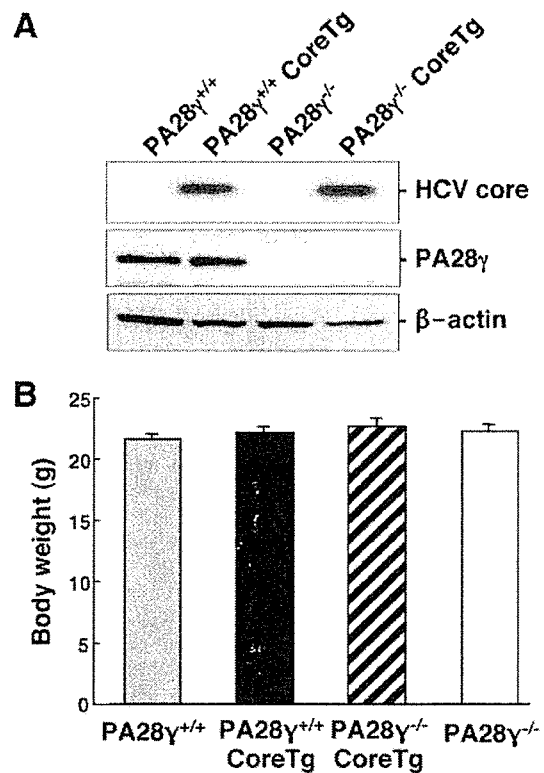

FIG. 1. Characterization of HCV core gene-transgenic mice deficient in the PA28γ gene. (A) Expression of the HCV core protein and PA28γ in the livers of PA28$\gamma^{+/+}$, PA28$\gamma^{+/+}$CoreTg, PA28$\gamma^{-/-}$, and PA28$\gamma^{-/-}$CoreTg mice. Lysates obtained from liver tissues of the mice (100 μg protein/lane) were subjected to sodium dodecyl sulfate-polyacrylamide gel electrophoresis and immunoblotting using antibodies to the HCV core protein, PA28γ, and β-actin. (B) Body weights of the mice. Body weights of 2-month-old mice were measured ($n = 7$ in each group). There were no statistically significant differences in body weights among the mice ($P > 0.05$).

CTCTGAGACCTTCTCAGCACCTAC-3' (forward) and 5'-GGAGTTGCCCT CATTGCTGCCTAA-3' (reverse) for IRS1, 5'-AGCCTGGGGATAATGGTG ACTATACCGA-3' (forward) and 5'-TTGTGGGCAAAGGATGGGGACAC T-3' (reverse) for IRS2, and 5'-CCAGCAAGCTTGCAACCTTAACCA-3' (forward) and 5'-GTAATGATCAGTCAACGGGGGAC-3' (reverse) for hypoxanthine phosphoribosyl transferase. Each PCR product was found as a single band with the correct size by agarose gel electrophoresis (data not shown).

Reporter assay for TNF-α promoter activity. The promoter region of the TNF-α gene (located from residues -1260 to $+140$) was amplified from mouse genomic DNA and was then introduced into the KpnI and BglII sites of pGL3-Basic (Promega, Madison, WI) (25). The resulting plasmid was designated as pGL3-tnf-aPro. The gene encoding the HCV core protein was amplified from HCV strain J1 (genotype 1b) and cloned into pCAG-GS (1, 38). To avoid contamination with endotoxin from *Escherichia coli*, the plasmid DNA was purified by using an EndoFree Plasmid Maxi kit (QIAGEN). The total amount of transfected DNA was normalized by the addition of empty plasmids. Plasmid vector was transfected into hepatoma cell lines by lipofection using Lipofectamine 2000 (Invitrogen). Cells were harvested at 24 h posttransfection. Luciferase activity was determined by using the Dual-Luciferase Reporter Assay system (Promega). Firefly luciferase activity was normalized to coexpressed *Renilla* luciferase activity. The amount of firefly luciferase activity was presented as the increase (n-fold) relative to the value for the sample lacking the HCV core protein, which was taken to be 1.0. PA28γ-knockdown cell lines were established by using pSilencer 2.1 U6 Hygro (Ambion) according to the manufacturer's protocol.
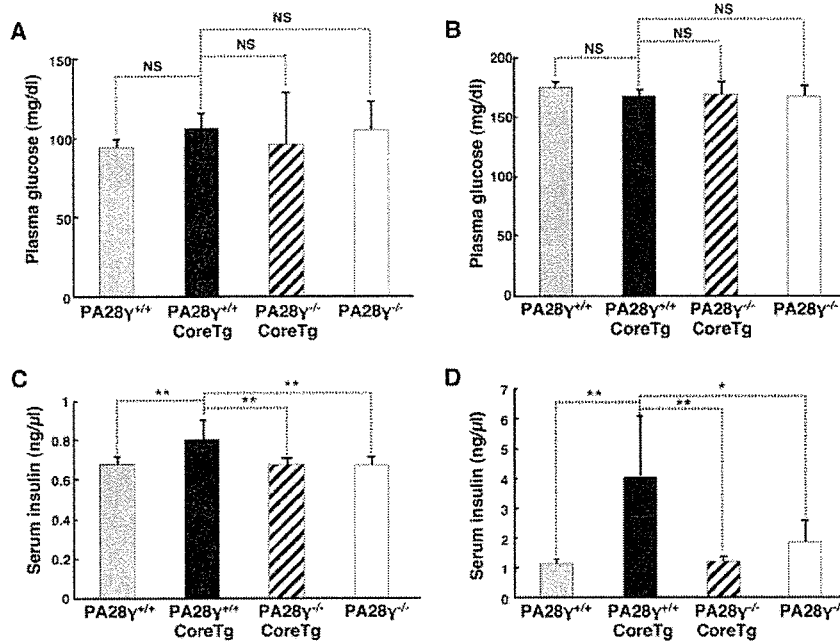
FIG. 2. Knockout of the PA28γ gene inhibited the hyperinsulinemia induced by HCV core protein. Plasma glucose levels of PA28$\gamma^{+/+}$, PA28$\gamma^{+/+}$CoreTg, PA28$\gamma^{-/-}$CoreTg, and PA28$\gamma^{-/-}$ mice under fasting (A) or fed (B) conditions ($n = 7$ in each group) are shown. Serum insulin levels in fasting (C) or fed (D) mice ($n = 7$ in each group) are also shown. Values are represented as means ± standard deviations. $*P < 0.05$; $**P < 0.01$. NS, not statistically significant.

Statistical analysis. The results are presented as means ± standard deviations. The significance of the differences was determined by Student's t test. P values of <0.05 were considered statistically significant.

RESULTS

HCV core gene-transgenic mice deficient in the PA28γ gene. To investigate the role of PA28γ in the development of insulin resistance in HCV core gene-transgenic (PA28$\gamma^{+/+}$CoreTg)

mice, we generated HCV core gene-transgenic mice deficient in the PA28γ gene (PA28$\gamma^{-/-}$CoreTg). A PA28$\gamma^{+/+}$CoreTg mouse expressing an amount of PA28γ equal to that of its normal littermates (Fig. 1A) was crossbred with a PA28$\gamma^{-/-}$ mouse to generate a PA28$\gamma^{+/-}$ CoreTg mouse. PA28$\gamma^{+/-}$ CoreTg mice were bred with each other, and a PA28$\gamma^{-/-}$ CoreTg mouse was selected by PCR. The HCV core protein was expressed in PA28$\gamma^{+/+}$CoreTg and PA28$\gamma^{-/-}$CoreTg

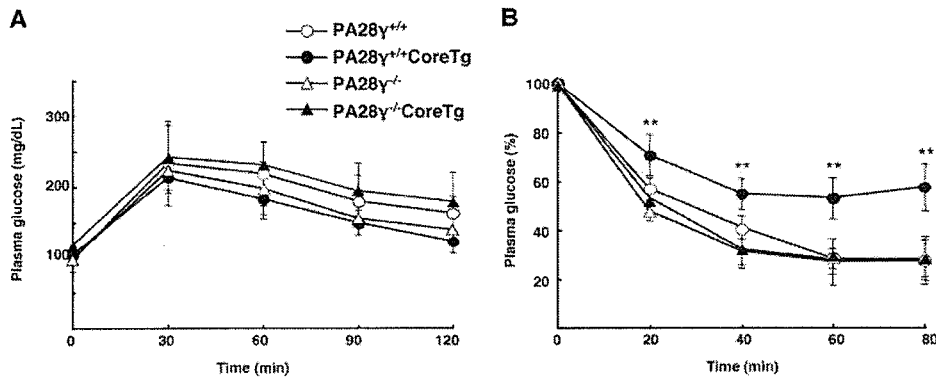FIG. 3. Knockout of the PA28γ gene inhibits the insulin resistance induced by the HCV core protein. (A) Glucose tolerance test. D-Glucose was intraperitoneally administered to mice fasted for more than 16 h at 1 g/kg of body weight. Plasma glucose levels were estimated at the indicated times ($n = 5$ in each group). There were no significant differences in glucose levels among the mice ($P > 0.05$). (B) Insulin tolerance test. Human insulin (2 units/kg body weight) was intraperitoneally administered to the mice, and the plasma glucose levels were estimated at the indicated times. Values were normalized to the baseline glucose concentration at the time of insulin administration ($n = 5$ in each group). The values for the PA28$\gamma^{+/+}$ (open circles), PA28$\gamma^{+/+}$CoreTg (closed circles), PA28$\gamma^{-/-}$ (open triangles), and PA28$\gamma^{-/-}$CoreTg (closed triangles) mice are represented as means and ± standard deviations. Significant differences in insulin sensitivity ($P < 0.01$) in PA28$\gamma^{+/+}$CoreTg mice compared to that in PA28$\gamma^{+/+}$, PA28$\gamma^{-/-}$, or PA28$\gamma^{-/-}$CoreTg mice are indicated by double asterisks ($**$). There were no significant differences among PA28$\gamma^{+/+}$, PA28$\gamma^{-/-}$, and PA28$\gamma^{-/-}$CoreTg mice ($P > 0.05$).
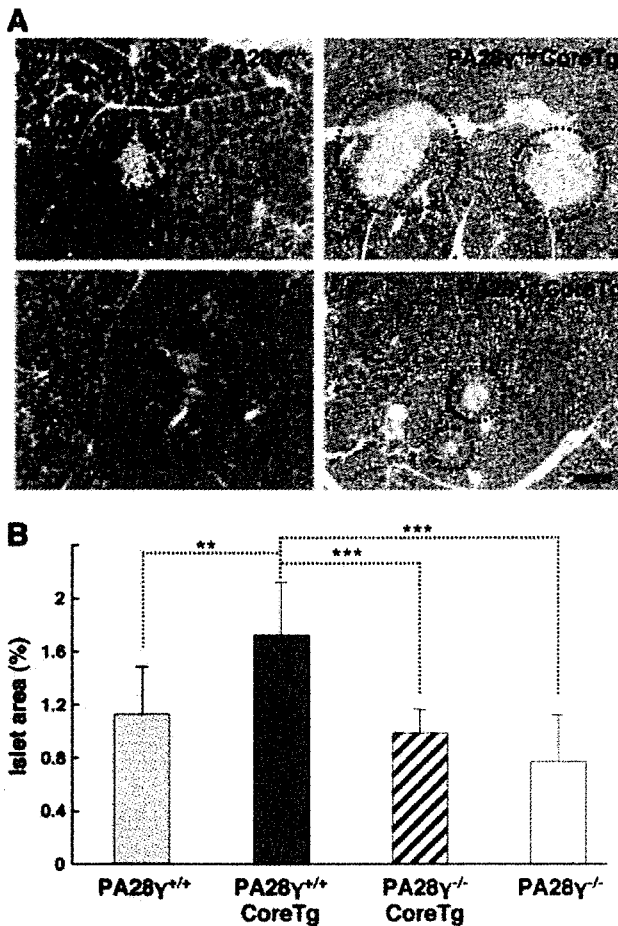
A

B

FIG. 4. PA28γ participated in the enlargement of pancreatic islets induced by the HCV core protein. (A) Histological sections prepared from pancreas tissues of PA28$\gamma^{+/+}$, PA28$\gamma^{+/+}$CoreTg, PA28$\gamma^{-/-}$, and PA28$\gamma^{-/-}$CoreTg mice were stained with hematoxylin and eosin. Dotted circles indicate pancreatic islets. (B) The area occupied by pancreatic islets was measured by computer software in three different fields of every six randomly selected sections of 10 mice per genotype and is represented as a percentage of the total pancreatic area. $**P < 0.01$; $***P < 0.001$. The scale bar indicates 100 μm.

A

B

FIG. 5. PA28γ participated in the inhibition of the tyrosine phosphorylation of IRS1 induced by the HCV core protein. Liver tissues from PA28$\gamma^{+/+}$, PA28$\gamma^{+/+}$CoreTg, PA28$\gamma^{-/-}$, and PA28$\gamma^{-/-}$CoreTg mice were prepared after administration of insulin (+) or phosphate-buffered saline (−). The samples (100 μg of total protein) were examined by immunoblotting with antibodies against IRS1 and phospho-Tyr608 of mouse IRS1 (A). Phosphorylated IRS1 was estimated from the density on the immunoblotted membrane by using computer software (B) ($n = 5$ in each group). The data presented are representative of three independent experiments. $*P < 0.05$; $**P < 0.01$.

mice but not in PA28$\gamma^{+/+}$ (normal littermates) or PA28$\gamma^{-/-}$ mice. PA28γ was found at a similar level in PA28$\gamma^{+/+}$CoreTg and PA28$\gamma^{+/+}$ mice but was not present in either PA28$\gamma^{-/-}$ or PA28$\gamma^{-/-}$CoreTg mice (Fig. 1A). The expression of the HCV core protein in the livers of 2-month-old male mice was slightly higher in PA28$\gamma^{-/-}$CoreTg (1.36 ± 0.44 ng/mg of total protein; $n = 7$) than in PA28$\gamma^{+/+}$CoreTg (1.23 ± 0.22 ng/mg of total protein; $n = 7$) mice, but these values were not significantly different ($P > 0.05$). Insulin sensitivity is dependent on several conditions such as body weight, obesity, and liver steatosis (26). PA28$\gamma^{-/-}$ mice were slightly smaller than their normal littermates (PA28$\gamma^{+/+}$) at more than 3 months old, as described previously (36), but this was not significantly different in 2-month-old mice (Fig. 1B). PA28$\gamma^{+/+}$CoreTg mice exhibited severe hepatic steatosis from 4 months of age (35). To avoid the influence of hepatic steatosis and body weight on the examination of insulin resistance, 2-month-old mice were
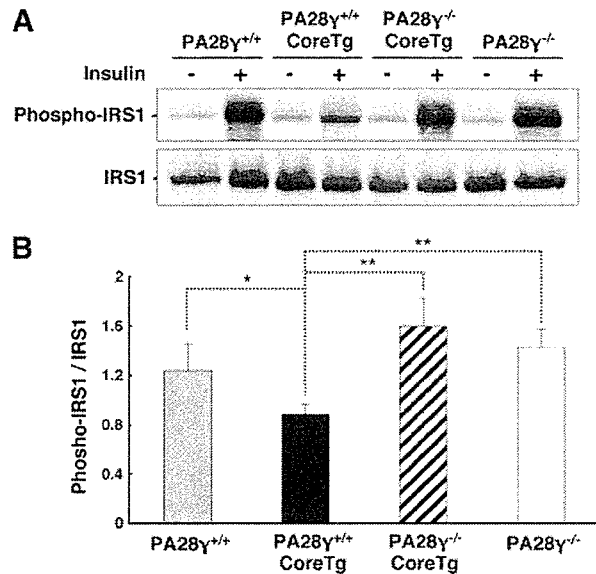
used in this study. Figure 1B shows the body weights of 2-month-old mice. There were no significant differences in body weight among PA28$\gamma^{+/+}$CoreTg, PA28$\gamma^{-/-}$CoreTg, PA28$\gamma^{-/-}$, and PA28$\gamma^{+/+}$ mice. Steatosis was not detected in the livers of the 2-month-old mice (data not shown).

PA28γ is involved in the development of hyperinsulinemia and insulin resistance in PA28$\gamma^{+/+}$CoreTg mice. In our previous study, we found a significant difference in serum insulin levels, but not in plasma glucose levels, between PA28$\gamma^{+/+}$ CoreTg mice and normal littermates (47). To determine the involvement of PA28γ in the development of insulin resistance in PA28$\gamma^{+/+}$CoreTg mice, we examined here the plasma glucose and insulin levels in the mice under fasting and fed conditions. Although no significant difference in plasma glucose levels was observed in the mice under either fasting (Fig. 2A) or fed (Fig. 2B) conditions, serum insulin levels were significantly higher in PA28$\gamma^{+/+}$CoreTg mice than in PA28$\gamma^{+/+}$ mice under both conditions (Fig. 2C and D), as described previously (47). In contrast, the serum insulin concentration in PA28$\gamma^{-/-}$CoreTg mice was recovered to a normal level similar to that of PA28$\gamma^{+/+}$ and PA28$\gamma^{-/-}$ mice under either fasting (Fig. 2C) or fed (Fig. 2D) conditions.

To determine the glucose intolerance among the mice, glucose was administered to the mice after fasting, and the plasma glucose level was then determined. There was no significant difference among the genotypes at any time point in the glucose tolerance test (Fig. 3A), suggesting that the volume of glucose was maintained at a normal level by the higher concentration of insulin in PA28$\gamma^{+/+}$CoreTg mice. In our previ-
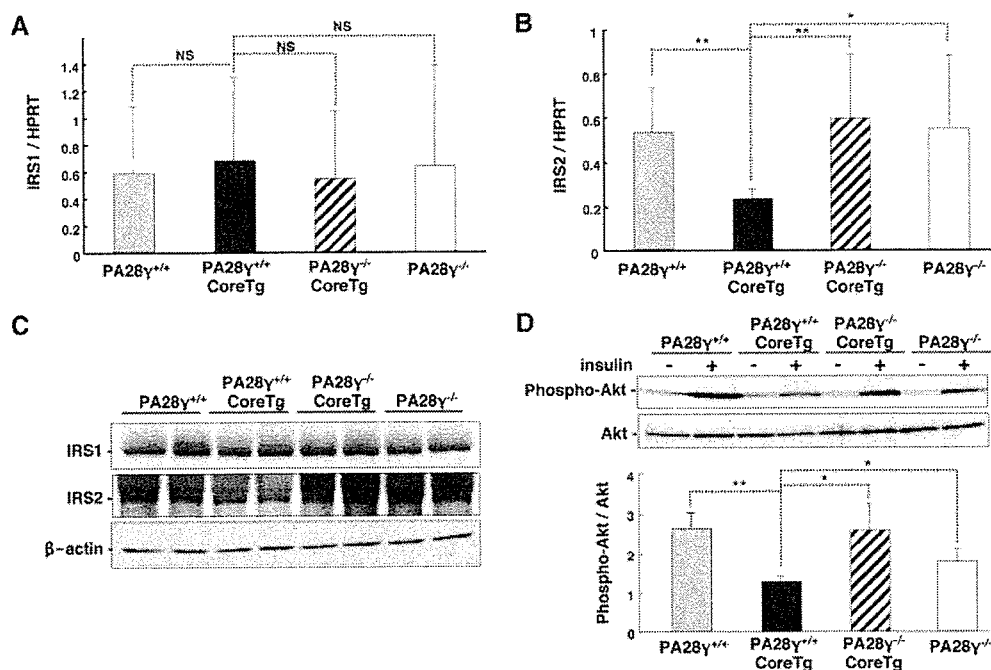
FIG. 6. PA28γ participated in the inhibition of the IRS2 expression and Akt phosphorylation induced by HCV core protein. The transcription of IRS1 (A) and IRS2 (B) was estimated by quantitative RT-PCR ($n = 5$ in each group). (C) The expression levels of IRS1 and IRS2 in the livers of the mice were determined by immunoblotting with specific antibodies. (D) Phosphorylation of Akt in the livers of the mice was examined by immunoblotting with antibodies against Akt and phosphorylated Akt. The ratio of Akt phosphorylation was determined by computer software based on the densities of phosphorylated Akt and a total amount of Akt ($n = 3$ in each group). The data presented are representative of three independent experiments. $*P < 0.05$; $**P < 0.01$. NS, not statistically significant; HPRT, hypoxanthine phosphoribosyl transferase.

ous study, the reduction in the plasma glucose concentration after insulin administration was impaired in PA28γ$^{+/+}$CoreTg mice (47). In this study, PA28γ$^{-/-}$CoreTg mice exhibited a normal insulin level comparable to those of PA28γ$^{+/+}$ and PA28γ$^{-/-}$ mice by an insulin tolerance test, in contrast to PA28γ$^{+/+}$CoreTg mice, in which a high concentration of plasma glucose was detected at all time points, as previously reported (Fig. 3B). These data suggest that hyperinsulinemia was induced in PA28γ$^{+/+}$CoreTg mice to compensate for insulin resistance and retain a physiological level of plasma glucose and that PA28γ participates in the development of hyperinsulinemia and insulin resistance in PA28γ$^{+/+}$CoreTg mice.

Morphology of pancreatic islets. Hyperinsulinemia and insulin resistance are expected to enlarge the pancreatic islet mass due to the overexpression of insulin. Our previous report showed the enlargement of the pancreatic islets in PA28γ$^{+/+}$ CoreTg mice. To clarify whether a knockout of the PA28γ gene restores the enlarged pancreatic islets to their normal size, the morphology of the pancreatic islets of the mice was evaluated by histologic examination (Fig. 4A). The relative islet area in the pancreatic cells of the PA28γ$^{-/-}$CoreTg mice was smaller than that of PA28γ$^{+/+}$CoreTg mice and comparable to that of PA28γ$^{+/+}$ and PA28γ$^{-/-}$ mice (Fig. 4B). Infiltration of inflammatory cells within or surrounding the islets was not found in all genotypes of mice. These results suggest that PA28γ also participates in the enlargement of pancreatic islets induced in PA28γ$^{+/+}$CoreTg mice.

PA28γ impairs the insulin-signaling pathway through the suppression of both tyrosine phosphorylation of IRS1 and expression of IRS2. Insulin binds to insulin receptors, resulting in the activation of downstream signaling (26). The activated insulin receptors phosphorylate themselves, IRS1, and IRS2. Phosphorylated IRS1 and IRS2 can activate phosphatidyl-inositol 3 (PI3)-kinase signaling, leading to the activation of glucose metabolism and cell growth. Our previous report showed that tyrosine phosphorylation of IRS1 is suppressed in the livers of PA28γ$^{+/+}$CoreTg mice and that the administration of anti-TNF-α antibody restores insulin sensitivity (47). We examined whether a knockout of the PA28γ gene could restore the tyrosine phosphorylation of IRS1. Tyrosine phosphorylation of IRS1 was suppressed in the livers of PA28γ$^{+/+}$ CoreTg mice in response to insulin stimulation, whereas it was recovered in PA28γ$^{-/-}$CoreTg mice to levels comparable to those in PA28γ$^{+/+}$and PA28γ$^{-/-}$ mice (Fig. 5).

Chronic hyperinsulinemia downregulates the expression of IRS2, which is one of the essential components of the insulin-signaling pathway in the liver (46). However, in our previous study, we showed that there was no significant difference in the phosphorylation of IRS2 between PA28γ$^{+/+}$CoreTg mice and their normal littermates (47). To gain more insight into the mechanisms of regulation of IRS expression, we determined the transcription and translation of IRS1 and IRS2 in the livers of the mice by real-time PCR and Western blotting, respectively. Although there was no significant difference in IRS1 expression at either the transcriptional or translational level among the mice
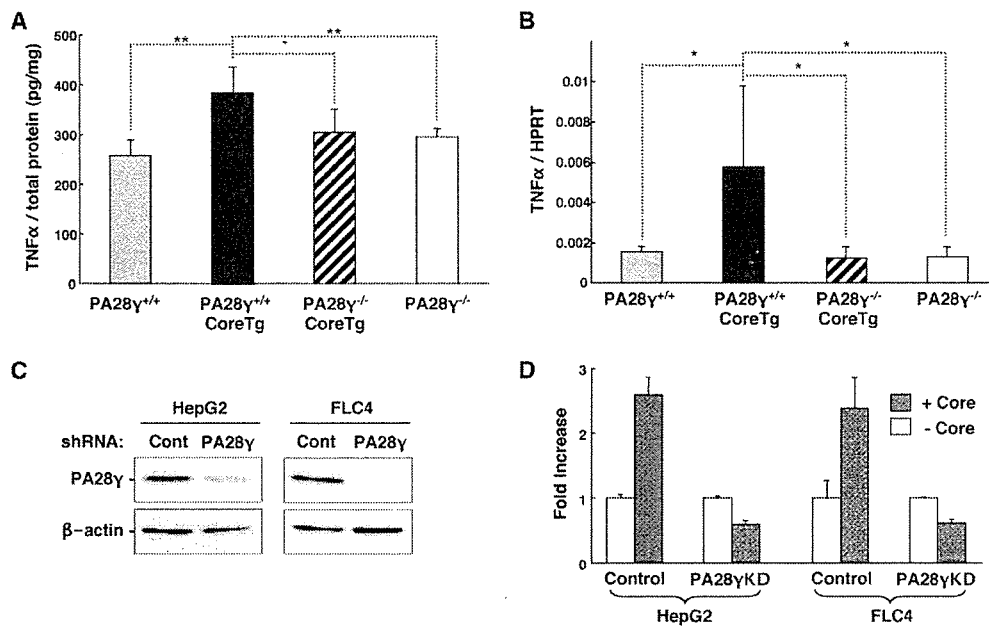
FIG. 7. PA28γ was required for activation of the TNF-α promoter by the HCV core protein. (A) Expression of TNF-α in the livers of mice was determined by ELISA ($n = 5$ in each group). (B) TNF-α mRNA in the livers of mice was examined by quantitative RT-PCR ($n = 5$ in each group). (C) Knockdown of the expression of PA28γ in the HepG2 and FLC-4 cell lines by the introduction of a plasmid encoding a short hairpin RNA (shRNA) targeted to the PA28γ gene. The expression levels of PA28γ and β-actin were determined by immunoblotting with specific antibodies. (D) Promoter activity of TNF-α in the presence or absence of the HCV core protein was determined by luciferase assay in the PA28γ-knockdown and control cell lines. The data presented are representative of three independent experiments. HPRT, hypoxanthine phosphoribosyl transferase.

(Fig. 6A and C), the expression of IRS2 was clearly impaired in PA28γ$^{+/+}$CoreTg mice at both the transcriptional and translational levels compared with that in other mice (Fig. 6B and C). The serine/threonine protein kinase Akt is phosphorylated by phosphoinositide-dependent kinase 1 (PDK1) under the activated condition of IRS family proteins (26). The insulin-induced phosphorylation of Akt was suppressed in the livers of PA28γ$^{+/+}$ CoreTg mice but not in those of PA28γ$^{+/+}$, PA28γ$^{-/-}$, or PA28γ$^{-/-}$CoreTg mice (Fig. 6D). These results suggest that the expression of the HCV core protein in the livers of mice in the presence of PA28γ impairs the insulin-signaling pathway through the suppression of both the tyrosine phosphorylation of IRS1 and the expression of IRS2.

PA28γ is required for activation of the TNF-α promoter by HCV core protein. TNF-α is an adipokine (54) and suppresses the signaling pathway of IRS1 and IRS2 (14, 42). Several reports suggested that the serum TNF-α level is higher in HCV patients than in healthy individuals (19, 37). Elevations of TNF-α levels have also been demonstrated in the livers of PA28γ$^{+/+}$CoreTg mice (47). To determine the involvement of PA28γ in the enhancement of TNF-α expression, the expression of TNF-α in the livers of each genotype was determined by ELISA and real-time PCR (Fig. 7A and B). Transcription and translation of TNF-α were increased in the livers of PA28γ$^{+/+}$ CoreTg mice but were restored in the livers of PA28γ$^{-/-}$ CoreTg mice to levels comparable to those of PA28γ$^{+/+}$ and PA28γ$^{-/-}$ mice. To determine the effect of PA28γ expression on the promoter activity of TNF-α in human liver cells, PA28γ-knockdown human hepatoma cell lines HepG2 and FLC4 were

established by the introduction of a plasmid encoding a short hairpin RNA targeting the PA28γ gene in the cell lines. The expression of PA28γ was clearly suppressed in the cell lines (Fig. 7C). The expression of HCV core protein in the hepatoma cell lines potentiated TNF-α promoter activity, whereas the promoter activation by the HCV core protein was suppressed in the PA28γ-knockdown cell lines (Fig. 7D). These results suggest that PA28γ is required for the activation of the TNF-α promoter induced by the expression of the HCV core protein in human hepatoma cell lines.

DISCUSSION

HCV infection has a close association with type 2 diabetes, which is a polygenic disease with a pathophysiology that includes a defect in insulin secretion, increased hepatic glucose production, and resistance to the action of insulin (2, 8, 18). Insulin binds to insulin receptors, which exhibit tyrosine kinase activity, leading to the autophosphorylation and phosphorylation of IRS (56). Tyrosine phosphorylation in IRS proteins leads to the interaction between IRS proteins and the regulatory subunit p85 of PI3-kinase, which enhances glucose uptake and inhibits lypolysis (21). Activated PI3-kinase phosphorylates phosphatidylinositol 4,5-biphosphate to produce phosphatidylinositol 3,4,5-triphosphate, which contributes to the activation of PDK1 (55). Activated PDK1 phosphorylates downstream substrates including Akt and other kinases (55). A diabetic phenotype that included insulin resistance was found in IRS2-knockout mice with normal growth (57), although a

knockout of the IRS1 gene has been shown to lead to growth retardation and insulin resistance but not overt diabetes (5, 52). The double knockdown of IRS1 and IRS2 genes in the liver induces hyperinsulinemia and insulin resistance in mice (53). The reduction of both IRS1 and IRS2 under conditions of insulin resistance and hyperinsulinemia (3) and in the livers of ob/ob mice, an obese diabetic mouse model (20), has been reported previously. In the present study, the expression of the HCV core protein reduced the phosphorylation of tyrosine on IRS1 and the production of IRS2 in the livers of mice but did not completely abolish the activities of these genes, suggesting that residual activities of IRS transfer a faint signal to the downstream region of IRS. Therefore, PA28γ$^{+/+}$CoreTg mice may exhibit a milder phenotype than IRS1- and/or IRS2-knockout mice. In this study, knockout of the PA28γ gene restored the insulin sensitivity and signaling of IRS1 and IRS2 in PA28γ$^{+/+}$CoreTg mice, suggesting that the expression of the HCV core protein leads to the dysfunction of both IRS1 and IRS2 through a PA28γ-dependent pathway.

Our previous study suggested that the induction of TNF-α by the HCV core protein plays a role in insulin resistance (47). An increase in TNF-α levels has been correlated with obesity and insulin resistance in animal models and humans (14, 42). However, the mechanism by which TNF-α induces insulin resistance is not completely known. The expression of TNF-α has been shown to be increased in PA28γ$^{+/+}$CoreTg mice, resulting in the suppression of phosphorylation of IRS1, and insulin sensitivity in PA28γ$^{+/+}$CoreTg was improved by the administration of an anti-TNF-α antibody (47). In the present study, the expression level of TNF-α in PA28γ$^{-/-}$CoreTg mice was similar to that in PA28γ$^{-/-}$ mice or their normal littermates. The expression of the HCV core protein enhanced the promoter activity of the TNF-α gene in human liver cell lines but not in those with a knockdown of the PA28γ gene by RNA interference (Fig. 7D). These data suggest that PA28γ plays a crucial role in HCV core-induced expression of TNF-α. Sterol regulatory element-binding proteins (SREBPs) were shown to be increased at the stage of viremia in HCV-infected chimpanzees (49). SREBPs are known to regulate not only the biosynthesis of lipid but also the transcription of IRS2 and TNF-α (17, 45). Therefore, it might be feasible to speculate that the HCV core protein may cooperate with PA28γ to regulate the expression of SREBPs.

Houstis et al. previously reported that reactive oxygen species (ROS) are increased in both cellular and mouse models of insulin resistance induced by treatment with TNF-α or dexamethasone and that insulin sensitivity was restored by treatment with small antioxidant molecules (16). The HCV core protein potentiates ROS production in hepatoma cells and HCV core gene-transgenic mice (23, 34, 41). Accelerated production of ROS results in mitochondrion dysfunction, which contributes to a decrease in fatty acid oxidation. Defects in mitochondrial fatty acid oxidation enhance the production of intracellular fatty acyl coenzyme A (CoA) and diacylglycerol (48, 58). Mitochondrion dysfunction and accumulation of lipid droplets in mice expressing the HCV core or the full-length HCV polyprotein have been reported (27, 34). An increase in lipid droplets also leads to the accumulation of fatty acid CoA and diacylglycerol (48, 58). Fatty acyl CoA and diacylglycerol nonspecifically activate the Ser/Thr kinase cascade, leading to the enhancement of the serine phosphorylation of IRS1 (26). Serine phosphorylation on IRS1 blocks the tyrosine

phosphorylation of IRS1 by insulin receptors (26). In the present study, however, serine phosphorylation of IRS1 in PA28γ$^{+/+}$CoreTg mice was similar to that in PA28γ$^{-/-}$CoreTg mice (data not shown). TNF-α signaling pathways other than the accumulation of ROS and fatty acid intermediates may also participate in the inhibition of tyrosine phosphorylation on IRS1 in PA28γ$^{+/+}$CoreTg mice.

How does the HCV core protein induce TNF-α production? Our previous report suggests that the HCV core protein is degraded through a PA28γ-dependent pathway (32). Recently, PA28γ has been shown to participate in the proteasome-dependent degradation of steroid receptor coactivator 3 (28). Degradation products of the HCV core protein via the PA28γ-dependent pathway may regulate the promoter activity of the TNF-α gene. PA28 proteins are necessary and sufficient to fully reconstitute Hsp90-initiated refolding together with Hsc70 and Hsp40 (31). Therefore, it might also be feasible to speculate that the HCV core protein refolded by an Hsp90/PA28γ-dependent pathway activates the promoter of the TNF-α gene together with an unknown transcription factor(s) or regulator(s).

In conclusion, the data obtained in this study suggest that the expression of the HCV core protein enhances the production of TNF-α and suppresses the phosphorylation of tyrosine on IRS1 and the production of IRS2 through a PA28γ-dependent pathway, thereby leading to insulin resistance. PA28γ may be a novel target for the treatment of HCV-induced diabetes.

REFERENCES

1. **Aizaki, H., Y. Aoki, T. Harada, K. Ishii, T. Suzuki, S. Nagamori, G. Toda, Y. Matsuura, and T. Miyamura.** 1998. Full-length complementary DNA of hepatitis C virus genome from an infectious blood sample. Hepatology **27:** 621–627.
2. **Allison, M. E., T. Wreghitt, C. R. Palmer, and G. J. Alexander.** 1994. Evidence for a link between hepatitis C virus infection and diabetes mellitus in a cirrhotic population. J. Hepatol. **21:**1135–1139.
3. **Anai, M., M. Funaki, T. Ogihara, J. Terasaki, K. Inukai, H. Katagiri, Y. Fukushima, Y. Yazaki, M. Kikuchi, Y. Oka, and T. Asano.** 1998. Altered expression levels and impaired steps in the pathway to phosphatidylinositol 3-kinase activation via insulin receptor substrates 1 and 2 in Zucker fatty rats. Diabetes **47:**13–23.
4. **Aoyagi, K., C. Ohue, K. Iida, T. Kimura, E. Tanaka, K. Kiyosawa, and S. Yagi.** 1999. Development of a simple and highly sensitive enzyme immunoassay for hepatitis C virus core antigen. J. Clin. Microbiol. **37:**1802–1808.
5. **Araki, E., M. A. Lipes, M. E. Patti, J. C. Bruning, B. Haag III, R. S. Johnson, and C. R. Kahn.** 1994. Alternative pathway of insulin signalling in mice with targeted disruption of the IRS-1 gene. Nature **372:**186–190.
6. **Bukh, J., R. H. Purcell, and R. H. Miller.** 1994. Sequence analysis of the core gene of 14 hepatitis C virus genotypes. Proc. Natl. Acad. Sci. USA **91:**8239–8243.
7. **Caronia, S., K. Taylor, L. Pagliaro, C. Carr, U. Palazzo, J. Petrik, S. O'Rahilly, S. Shore, B. D. Tom, and G. J. Alexander.** 1999. Further evidence for an association between non-insulin-dependent diabetes mellitus and chronic hepatitis C virus infection. Hepatology **30:**1059–1063.
8. **Cavaghan, M. K., D. A. Ehrmann, and K. S. Polonsky.** 2000. Interactions between insulin resistance and insulin secretion in the development of glucose intolerance. J. Clin. Investig. **106:**329–333.
9. **Choo, Q. L., G. Kuo, A. J. Weiner, L. R. Overby, D. W. Bradley, and M. Houghton.** 1989. Isolation of a cDNA clone derived from a blood-borne non-A, non-B viral hepatitis genome. Science **244:**359–362.

10. Choo, Q. L., K. H. Richman, J. H. Han, K. Berger, C. Lee, C. Dong, C. Gallegos, D. Coit, R. Medina-Selby, P. J. Barr, et al. 1991. Genetic organization and diversity of the hepatitis C virus. Proc. Natl. Acad. Sci. USA 88:2451–2455.

11. Falcon, V., N. Acosta-Rivero, G. Chinea, J. Gavilondo, M. C. de la Rosa, I. Menendez, S. Duenas-Carrera, A. Vina, W. Garcia, B. Gra, M. Noa, E. Reytor, M. T. Barcelo, F. Alvarez, and J. Morales-Grillo. 2003. Ultrastructural evidences of HCV infection in hepatocytes of chronically HCV-infected patients. Biochem. Biophys. Res. Commun. 305:1085–1090.

12. Grakoui, A., D. W. McCourt, C. Wychowski, S. M. Feinstone, and C. M. Rice. 1993. Characterization of the hepatitis C virus-encoded serine proteinase: determination of proteinase-dependent polyprotein cleavage sites. J. Virol. 67:2832–2843.

13. Gumber, S. C., and S. Chopra. 1995. Hepatitis C: a multifaceted disease. Review of extrahepatic manifestations. Ann. Intern. Med. 123:615–620.

14. Hotamisligil, G. S. 1999. The role of TNFalpha and TNF receptors in obesity and insulin resistance. J. Intern. Med. 245:621–625.

15. Houghton, M., A. Weiner, J. Han, G. Kuo, and Q. L. Choo. 1991. Molecular biology of the hepatitis C viruses: implications for diagnosis, development and control of viral disease. Hepatology 14:381–388.

16. Houstis, N., E. D. Rosen, and E. S. Lander. 2006. Reactive oxygen species have a causal role in multiple forms of insulin resistance. Nature 440:944–948.

17. Ide, T., H. Shimano, N. Yahagi, T. Matsuzaka, M. Nakakuki, T. Yamamoto, Y. Nakagawa, A. Takahashi, H. Suzuki, H. Sone, H. Toyoshima, A. Fukamizu, and N. Yamada. 2004. SREBPs suppress IRS-2-mediated insulin signalling in the liver. Nat. Cell Biol. 6:351–357.

18. Kahn, B. B. 1998. Type 2 diabetes: when insulin secretion fails to compensate for insulin resistance. Cell 92:593–596.

19. Kallinowski, B., K. Haseroth, G. Marinos, C. Hanck, W. Stremmel, L. Theilmann, M. V. Singer, and S. Rossol. 1998. Induction of tumour necrosis factor (TNF) receptor type p55 and p75 in patients with chronic hepatitis C virus (HCV) infection. Clin. Exp. Immunol. 111:269–277.

20. Kerouz, N. J., D. Horsch, S. Pons, and C. R. Kahn. 1997. Differential regulation of insulin receptor substrates-1 and -2 (IRS-1 and IRS-2) and phosphatidylinositol 3-kinase isoforms in liver and muscle of the obese diabetic (ob/ob) mouse. J. Clin. Investig. 100:3164–3172.

21. Kido, Y., J. Nakae, and D. Accili. 2001. Clinical review 125: the insulin receptor and its cellular targets. J. Clin. Endocrinol. Metab. 86:972–979.

22. Kiyosawa, K., T. Sodeyama, E. Tanaka, Y. Gibo, K. Yoshizawa, Y. Nakano, S. Furuta, Y. Akahane, K. Nishioka, R. H. Purcell, et al. 1990. Interrelationship of blood transfusion, non-A, non-B hepatitis and hepatocellular carcinoma: analysis by detection of antibody to hepatitis C virus. Hepatology 12:671–675.

23. Korenaga, M., T. Wang, Y. Li, L. A. Showalter, T. Chan, J. Sun, and S. A. Weinman. 2005. Hepatitis C virus core protein inhibits mitochondrial electron transport and increases reactive oxygen species (ROS) production. J. Biol. Chem. 280:37481–37488.

24. Kuo, G., Q. L. Choo, H. J. Alter, G. L. Gitnick, A. G. Redeker, R. H. Purcell, T. Miyamura, J. L. Dienstag, M. J. Alter, C. E. Stevens, et al. 1989. An assay for circulating antibodies to a major etiologic virus of human non-A, non-B hepatitis. Science 244:362–364.

25. Kuprash, D. V., I. A. Udalova, R. L. Turetskaya, D. Kwiatkowski, N. R. Rice, and S. A. Nedospasov. 1999. Similarities and differences between human and murine TNF promoters in their response to lipopolysaccharide. J. Immunol. 162:4045–4052.

26. Lazar, D. F., and A. R. Saltiel. 2006. Lipid phosphatases as drug discovery targets for type 2 diabetes. Nat. Rev. Drug Discov. 5:333–342.

27. Lerat, H., M. Honda, M. R. Beard, K. Loesch, J. Sun, Y. Yang, M. Okuda, R. Gosert, S. Y. Xiao, S. A. Weinman, and S. M. Lemon. 2002. Steatosis and liver cancer in transgenic mice expressing the structural and nonstructural proteins of hepatitis C virus. Gastroenterology 122:352–365.

28. Li, X., D. M. Lonard, S. Y. Jung, A. Malovannaya, Q. Feng, J. Qin, S. Y. Tsai, M. J. Tsai, and B. W. O'Malley. 2006. The SRC-3/AIB1 coactivator is degraded in a ubiquitin- and ATP-independent manner by the REGgamma proteasome. Cell 124:381–392.

29. Mason, A. L., J. Y. Lau, N. Hoang, K. Qian, G. J. Alexander, L. Xu, L. Guo, S. Jacob, F. G. Regenstein, R. Zimmerman, J. E. Everhart, C. Wasserfall, N. K. Maclaren, and R. P. Perrillo. 1999. Association of diabetes mellitus and chronic hepatitis C virus infection. Hepatology 29:328–333.

30. McLauchlan, J., M. K. Lemberg, G. Hope, and B. Martoglio. 2002. Intramembrane proteolysis promotes trafficking of hepatitis C virus core protein to lipid droplets. EMBO J. 21:3980–3988.

31. Minami, Y., H. Kawasaki, M. Minami, N. Tanahashi, K. Tanaka, and I. Yahara. 2000. A critical role for the proteasome activator PA28 in the Hsp90-dependent protein refolding. J. Biol. Chem. 275:9055–9061.

32. Moriishi, K., T. Okabayashi, K. Nakai, K. Moriya, K. Koike, S. Murata, T. Chiba, K. Tanaka, R. Suzuki, T. Suzuki, T. Miyamura, and Y. Matsuura. 2003. Proteasome activator PA28γ-dependent nuclear retention and degradation of hepatitis C virus core protein. J. Virol. 77:10237–10249.

33. Moriya, K., H. Fujie, Y. Shintani, H. Yotsuyanagi, T. Tsutsumi, K. Ishibashi, Y. Matsuura, S. Kimura, T. Miyamura, and K. Koike. 1998. The core protein

34. Moriya, K., K. Nakagawa, T. Santa, Y. Shintani, H. Fujie, H. Miyoshi, T. Tsutsumi, T. Miyazawa, K. Ishibashi, T. Horie, K. Imai, T. Todoroki, S. Kimura, and K. Koike. 2001. Oxidative stress in the absence of inflammation in a mouse model for hepatitis C virus-associated hepatocarcinogenesis. Cancer Res. 61:4365–4370.

35. Moriya, K., H. Yotsuyanagi, Y. Shintani, H. Fujie, K. Ishibashi, Y. Matsuura, T. Miyamura, and K. Koike. 1997. Hepatitis C virus core protein induces hepatic steatosis in transgenic mice. J Gen. Virol. 78:1527–1531.

36. Murata, S., H. Kawahara, S. Tohma, K. Yamamoto, M. Kasahara, Y. Nabeshima, K. Tanaka, and T. Chiba. 1999. Growth retardation in mice lacking the proteasome activator PA28gamma. J. Biol. Chem. 274:38211–38215.

37. Nelson, D. R., H. L. Lim, C. G. Marousis, J. W. Fang, G. L. Davis, L. Shen, M. S. Urdea, J. A. Kolberg, and J. Y. Lau. 1997. Activation of tumor necrosis factor-alpha system in chronic hepatitis C virus infection. Dig. Dis. Sci. 42:2487–2494.

38. Niwa, H., K. Yamamura, and J. Miyazaki. 1991. Efficient selection for high-expression transfectants with a novel eukaryotic vector. Gene 108:193–199.

39. Ogino, T., H. Fukuda, S. Imajoh-Ohmi, M. Kohara, and A. Nomoto. 2004. Membrane binding properties and terminal residues of the mature hepatitis C virus capsid protein in insect cells. J. Virol. 78:11766–11777.

40. Okamoto, K., K. Moriishi, T. Miyamura, and Y. Matsuura. 2004. Intramembrane proteolysis and endoplasmic reticulum retention of hepatitis C virus core protein. J. Virol. 78:6370–6380.

41. Okuda, M., K. Li, M. R. Beard, L. A. Showalter, F. Scholle, S. M. Lemon, and S. A. Weinman. 2002. Mitochondrial injury, oxidative stress, and antioxidant gene expression are induced by hepatitis C virus core protein. Gastroenterology 122:366–375.

42. Ozes, O. N., H. Akca, L. D. Mayo, J. A. Gustin, T. Maehama, J. E. Dixon, and D. B. Donner. 2001. A phosphatidylinositol 3-kinase/Akt/mTOR pathway mediates and PTEN antagonizes tumor necrosis factor inhibition of insulin signaling through insulin receptor substrate-1. Proc. Natl. Acad. Sci. USA 98:4640–4645.

43. Rui, L., T. L. Fisher, J. Thomas, and M. F. White. 2001. Regulation of insulin/insulin-like growth factor-1 signaling by proteasome-mediated degradation of insulin receptor substrate-2. J. Biol. Chem. 276:40362–40367.

44. Shimoike, T., S. Mimori, H. Tani, Y. Matsuura, and T. Miyamura. 1999. Interaction of hepatitis C virus core protein with viral sense RNA and suppression of its translation. J. Virol. 73:9718–9725.

45. Shimomura, I., R. E. Hammer, J. A. Richardson, S. Ikemoto, Y. Bashmakov, J. L. Goldstein, and M. S. Brown. 1998. Insulin resistance and diabetes mellitus in transgenic mice expressing nuclear SREBP-1c in adipose tissue: model for congenital generalized lipodystrophy. Genes Dev. 12:3182–3194.

46. Shimomura, I., M. Matsuda, R. E. Hammer, Y. Bashmakov, M. S. Brown, and J. L. Goldstein. 2000. Decreased IRS-2 and increased SREBP-1c lead to mixed insulin resistance and sensitivity in livers of lipodystrophic and ob/ob mice. Mol. Cell 6:77–86.

47. Shintani, Y., H. Fujie, H. Miyoshi, T. Tsutsumi, K. Tsukamoto, S. Kimura, K. Moriya, and K. Koike. 2004. Hepatitis C virus infection and diabetes: direct involvement of the virus in the development of insulin resistance. Gastroenterology 126:840–848.

48. Shulman, G. I. 2000. Cellular mechanisms of insulin resistance. J. Clin. Investig. 106:171–176.

49. Su, A. I., J. P. Pezacki, L. Wodicka, A. D. Brideau, L. Supekova, R. Thimme, S. Wieland, J. Bukh, R. H. Purcell, P. G. Schultz, and F. V. Chisari. 2002. Genomic analysis of the host response to hepatitis C virus infection. Proc. Natl. Acad. Sci. USA 99:15669–15674.

50. Sun, X. J., J. L. Goldberg, L. Y. Qiao, and J. J. Mitchell. 1999. Insulin-induced insulin receptor substrate-1 degradation is mediated by the proteasome degradation pathway. Diabetes 48:1359–1364.

51. Suzuki, R., S. Sakamoto, T. Tsutsumi, A. Rikimaru, K. Tanaka, T. Shimoike, K. Moriishi, T. Iwasaki, K. Mizumoto, Y. Matsuura, T. Miyamura, and T. Suzuki. 2005. Molecular determinants for subcellular localization of hepatitis C virus core protein. J. Virol. 79:1271–1281.

52. Tamemoto, H., T. Kadowaki, K. Tobe, T. Yagi, H. Sakura, T. Hayakawa, Y. Terauchi, K. Ueki, Y. Kaburagi, S. Satoh, et al. 1994. Insulin resistance and growth retardation in mice lacking insulin receptor substrate-1. Nature 372:182–186.

53. Taniguchi, C. M., K. Ueki, and R. Kahn. 2005. Complementary roles of IRS-1 and IRS-2 in the hepatic regulation of metabolism. J. Clin. Investig. 115:718–727.

54. Uysal, K. T., S. M. Wiesbrock, M. W. Marino, and G. S. Hotamisligil. 1997. Protection from obesity-induced insulin resistance in mice lacking TNF-alpha function. Nature 389:610–614.

55. Vanhaesebroeck, B., and D. R. Alessi. 2000. The PI3K-PDK1 connection: more than just a road to PKB. Biochem. J. 346:561–576.

56. White, M. F. 1998. The IRS-signalling system: a network of docking proteins that mediate insulin action. Mol. Cell. Biochem. 182:3–11.
57. Withers, D. J., J. S. Gutierrez, H. Towery, D. J. Burks, J. M. Ren, S. Previs, Y. Zhang, D. Bernal, S. Pons, G. I. Shulman, S. Bonner-Weir, and M. F. White. 1998. Disruption of IRS-2 causes type 2 diabetes in mice. Nature 391:900–904.

58. Yu, C., Y. Chen, G. W. Cline, D. Zhang, H. Zong, Y. Wang, R. Bergeron, J. K. Kim, S. W. Cushman, G. J. Cooney, B. Atcheson, M. F. White, E. W. Kraegen, and G. I. Shulman. 2002. Mechanism by which fatty acids inhibit insulin activation of insulin receptor substrate-1 (IRS-1)-associated phosphatidylinositol 3-kinase activity in muscle. J. Biol. Chem. 277: 50230–50236.

E6AP Ubiquitin Ligase Mediates Ubiquitylation and Degradation of Hepatitis C Virus Core Protein[∇]

Masayuki Shirakura,[1] Kyoko Murakami,[1] Tohru Ichimura,[2] Ryosuke Suzuki,[1] Tetsu Shimoji,[1]
Kouichirou Fukuda,[1] Katsutoshi Abe,[1] Shigeko Sato,[3] Masayoshi Fukasawa,[3]
Yoshio Yamakawa,[3] Masahiro Nishijima,[3] Kohji Moriishi,[4] Yoshiharu Matsuura,[4]
Takaji Wakita,[1] Tetsuro Suzuki,[1] Peter M. Howley,[5]
Tatsuo Miyamura,[1] and Ikuo Shoji[1]*

Department of Virology II[1] and Department of Biochemistry and Cell Biology,[3] National Institute of Infectious Diseases, Shinjuku-ku,
Tokyo 162-8640, Japan; Department of Chemistry, Graduate School of Science, Tokyo Metropolitan University, Hachioji-shi,
Tokyo 192-0397, Japan[2]; Department of Molecular Virology, Research Institute for Microbial Diseases, Osaka University,
Osaka 565-0871, Japan[4]; and Department of Pathology, Harvard Medical School, 77 Avenue Louis Pasteur,
Boston, Massachusetts 02115[5]

Hepatitis C virus (HCV) core protein is a major component of viral nucleocapsid and a multifunctional protein involved in viral pathogenesis and hepatocarcinogenesis. We previously showed that the HCV core protein is degraded through the ubiquitin-proteasome pathway. However, the molecular machinery for core ubiquitylation is unknown. Using tandem affinity purification, we identified the ubiquitin ligase E6AP as an HCV core-binding protein. E6AP was found to bind to the core protein in vitro and in vivo and promote its degradation in hepatic and nonhepatic cells. Knockdown of endogenous E6AP by RNA interference increased the HCV core protein level. In vitro and in vivo ubiquitylation assays showed that E6AP promotes ubiquitylation of the core protein. Exogenous expression of E6AP decreased intracellular core protein levels and supernatant HCV infectivity titers in the HCV JFH1-infected Huh-7 cells. Furthermore, knockdown of endogenous E6AP by RNA interference increased intracellular core protein levels and supernatant HCV infectivity titers in the HCV JFH1-infected cells. Taken together, our results provide evidence that E6AP mediates ubiquitylation and degradation of HCV core protein. We propose that the E6AP-mediated ubiquitin-proteasome pathway may affect the production of HCV particles through controlling the amounts of viral nucleocapsid protein.

Hepatitis C virus (HCV; a single-stranded, positive-sense RNA virus that is classified in the family *Flaviviridae*) is the main cause of chronic hepatitis, liver cirrhosis, and hepatocellular carcinoma (5, 26, 45). More than 170 million people worldwide are chronically infected with HCV (41). The approximately 9.6-kb HCV genome encodes a unique open reading frame that is translated into a polyprotein (5, 54). The polyprotein is cleaved cotranslationally into at least 10 proteins by viral proteases and cellular signalases (6, 10).

The HCV core protein represents the first 1 to 191 amino acids (aa) of the polyprotein and is followed by two glycoproteins, E1 and E2 (6). The core protein plays a central role in the packaging of viral RNA (25, 40); modulates various cellular processes, including signal transduction pathways, transcriptional control, cell cycle progression, apoptosis, lipid metabolism, and the immune response (9, 40); and has transforming potential in certain cells (43). Mice transgenic for the HCV core gene develop steatosis (32) and later hepatocellular carcinoma (31). These findings suggest that HCV core protein plays a crucial role in hepatocarcinogenesis.

Two major forms of the HCV core protein, p21 (mature form) and p23 (immature form), can be generated in cultured cells (60). Cellular signal peptidase cleaves at the junction of the core/E1, releasing the immature form of the core protein from the polypeptide (12, 46). Signal peptide peptidase cleaves just before the signal sequence, liberating the mature form of the HCV core protein at the cytoplasmic face of the endoplasmic reticulum (29). Several different sites have been proposed as potential cleavage sites of signal peptide peptidase, such as Leu-179 (15, 29), Phe-177 (36, 37), Leu-182 (15), and Ser-173 (46). Further processing of the HCV core protein yields a 17-kDa product with a C terminus at around amino acid 152. A truncated form of the core protein, p17, was found in transfected cells (42, 52) and liver tissues from humans with hepatocellular carcinoma (59). The majority of this protein translocates to the nucleus. The C terminus of the core protein is important for regulating the stability of the protein (20, 52).

We previously showed that the C-terminally truncated forms of the core protein are degraded through the ubiquitin-proteasome pathway (52). We found that the mature form of the core protein, p21, also links to a few ubiquitin moieties, suggesting that the ubiquitin-proteasome pathway involves proteolysis of heterologous species of the core protein (52). Overexpression of PA28γ (a REG family proteasome activator also known as REGγ or Ki antigen) enhances the proteasomal degradation of the HCV core protein (30). A recent study has shown that

* Corresponding author. Mailing address: Department of Virology II, National Institute of Infectious Diseases, 1-23-1 Toyama, Shinjuku-ku, Tokyo 162-8640, Japan. Phone: 81 3-5285-1111. Fax: 81 3-5285-1161. E-mail: ishoji@nih.go.jp.

PA28γ is involved in the degradation of the steroid receptor coactivator 3 (SRC-3) in an ATP- and ubiquitin-independent manner (27). It is still unclear what E3 ubiquitin ligase is responsible for ubiquitylation of the HCV core protein.

E6AP was initially identified as the cellular factor that stimulates ubiquitin-mediated degradation of the tumor suppressor p53 in conjunction with the E6 protein of cancer-associated human papillomavirus types 16 and 18 (14, 48). The E6-E6AP complex functions as a E3 ubiquitin ligase in the ubiquitylation of p53 (49). E6AP is the prototype of a family of ubiquitin ligases called HECT domain ubiquitin ligases, all of which contain a domain *homologous* to the *E6AP carboxyl terminus* (13). Interestingly, E6AP is not involved in the regulation of p53 ubiquitylation in the absence of E6 (55). Several potential E6-independent substrates for E6AP have been identified, such as hHR23A, Blk, and Mcm7 (23, 24, 35). E6AP is also a candidate gene for Angelman syndrome, which is a severe neurological disorder characterized by mental retardation (21).

This study aimed to identify endogenous ubiquitin-proteasome pathway proteins that are associated with HCV core protein. Tandem affinity purification and mass spectrometry analysis identified E6AP as an HCV core-binding protein. Here we present evidence that E6AP associates with HCV core protein in vitro and in vivo and is involved in ubiquitylation and degradation of HCV core protein. We propose that an E6AP-mediated ubiquitin-proteasome pathway may affect the production of HCV particles through controlling the amounts of HCV core protein.

MATERIALS AND METHODS

Cell culture and transfection. Human embryonic kidney 293T cells, human hepatoblastoma HepG2 cells, and human hepatoma Huh-7 cells were cultured in Dulbecco's modified Eagle's medium (Sigma) supplemented with 50 IU/ml penicillin, 50 µg/ml streptomycin (Invitrogen), and 10% (vol/vol) fetal bovine serum (JRH Biosciences) at 37°C in a 5% CO_2 incubator. 293T cells and HepG2 cells were transfected with plasmid DNA using FuGene 6 transfection reagents (Roche). Huh-7 cells were transfected with plasmid DNA using *Trans*IT LT1 transfection reagents (Mirus).

Plasmids and recombinant baculoviruses. MEF tag cassette (containing *myc* tag, the tobacco *etch* virus protease cleavage site, and *F*LAG tag) (16) was fused to the N terminus of the cDNA encoding core protein of HCV NIHJ1 (genotype 1b) (1). To express MEF-tagged core protein in mammalian cells, the genome coding for HCV core protein (amino acids 1 to 191) was amplified by PCR using pBR HCV NIHJ1 as a template. Sense oligonucleotide containing a Kozak consensus translation initiation codon and antisense oligonucleotide containing an in-frame translation stop codon were synthesized by PCR. The amplified PCR product was purified, digested with EcoRI and EcoRV, and then inserted into the EcoRI-EcoRV site of pcDNA3-MEF. FLAG-tagged HCV core expression plasmids based upon pCAGGS (34) were described previously (30). To express E6AP and the active-site cysteine-to-alanine mutant of E6AP in mammalian cells, pCMV4-HA-E6AP isoform II and pCMV4-HA-E6AP C-A were utilized (19). The C-A mutation was introduced at the site of E6AP C843. To express E6AP and E6AP C-A under the CAG promoter, the E6AP fragment and the E6AP C-A fragment were amplified by PCR, purified, digested with SmaI and NotI, and blunt ended using a DNA blunting kit (Takara). These PCR fragments were subcloned into pCAGGS.

To make a fusion protein consisting of glutathione S-transferase (GST) fused to the N terminus of E6AP in *Escherichia coli*, the E6AP fragment was amplified by PCR and the resultant product was cloned into the SmaI-NotI site of pGEX4T-1 vector (Amersham Biosciences). To express a series of E6AP truncation mutants as GST fusion proteins, each fragment was amplified by PCR and cloned into the SmaI-NotI site of pGEX4T-1. To purify GST core protein efficiently by two-step affinity purification, we fused hexahistidine (His) tag to the C terminus of GST fusion proteins. To bacterially express HCV core (aa 1 to 173) protein as a fusion protein containing N-terminal GST tag and C-terminal

His tag, core fragment was amplified by PCR and the resultant product was cloned into the EcoRI-NotI site of pGEX4T-1 vector. The resultant plasmid was designated pGEX GST-C173HT. To express GST core (1–152)-His and GST-His in *E. coli*, pGEX core (1–152)-His and pGEX-His were constructed similarly. The resultant plasmids were designated pGEX GST-C152HT and pGEX GST-HT, respectively.

To generate recombinant baculoviruses expressing GST-E6AP, GST-E6AP fragment was excised from pGEX E6AP by digestion with SmaI and Tth111I and ligated into the SmaI-Tth111I site of pVL1392 (Invitrogen). To express GST-E6AP C-A, pVLGST-E6AP C-A was constructed similarly. To generate recombinant baculovirus expressing HCV core (aa 1 to 173) protein as a fusion protein containing N-terminal GST tag and C-terminal His tag, GST-C173HT fragment was amplified by PCR using pGEX GST-C173HT as a template, digested with BglII-XbaI, and subcloned into the BglII-XbaI site of pVL1392. To generate recombinant baculoviruses expressing GST-C152HT and GST-HT, cDNA fragments corresponding to GST-C152HT and GST-HT were amplified by PCR and subcloned into pVL1392, respectively. The resultant plasmids were designated pVLGST-C173HT, pVLGST-C152HT, and pVLGST-HT. To generate recombinant baculovirus expressing MEF-tagged E6AP, cDNA fragment encoding MEF-E6AP was subcloned into pVL1392. To express HCV core protein in the TNT-coupled wheat germ lysate system (Promega), HCV core cDNA was inserted in the EcoRI site of pCMVTNT (Promega). The primer sequences used in this study are available from the authors upon request. The sequences of the inserts were extensively verified using an ABI PRISM 3100-Avant Genetic Analyzer (Applied Biosystems). Recombinant baculoviruses were recovered using a BaculoGold transfection kit (Pharmingen) according to the manufacturer's instructions.

Antibodies. The mouse monoclonal antibodies (MAbs) used in this study were anti-hemagglutinin (anti-HA) MAb (12CA5; Roche), anti-FLAG (M2) MAb (Sigma), anti-c-*myc* MAb (9E10; Santa Cruz), anti-glyceraldehyde-3-phosphate dehydrogenase (anti-GAPDH) MAb (Chemicon), anti-GST MAb (Santa Cruz), anti-ubiquitin MAb (Chemicon), anti-E6AP MAb (E6AP-330) (Sigma), anticore MAb (B2; Anogen), and another anti-core MAb (2H9) (56). Polyclonal antibodies (PAbs) used in this study were anti-HA rabbit PAb (Y-11; Santa Cruz), anti-FLAG rabbit PAb (F7425; Sigma), anti-E6AP rabbit PAb (H-182; Santa Cruz), anti-DDX3 rabbit PAb (47), anti-PA28γ rabbit PAb (Affiniti), and anti-GST goat PAb (Amersham). Anticore rabbit PAb (TS1) was raised against the recombinant GST core protein.

MEF purification procedure. 293T cells were transfected with the plasmid expressing MEF core by the calcium phosphate precipitation method (4). After the cells were lysed, the expressed MEF core and its binding proteins were recovered following the procedure described previously (16). 293T cells transfected with pcDNA3-MEF core in four 10-cm dishes were lysed in 2 ml of lysis buffer: 50 mM Tris-HCl (pH 7.5), 150 mM NaCl, 10% (wt/vol) glycerol, 100 mM NaF, 1 mM Na_3VO_4, 1% (wt/vol) Triton X-100, 5 µM $ZnCl_2$, 2 mM phenylmethylsulfonyl fluoride, 10 µg/ml aprotinin, and 1 µg/ml leupeptin. The lysate was centrifuged at 100,000 × *g* for 20 min at 4°C. The supernatant was passed through a 5-µm filter, incubated with 100 µl of Sepharose beads for 60 min at 4°C, and then passed through a 0.65-µm filter. The filtered supernatant was mixed with 100 µl of anti-myc-conjugated Sepharose beads for the first immunoprecipitation. After incubation for 90 min at 4°C, the beads were washed five times with 1 ml of TNTG buffer (20 mM Tris-HCl, pH 7.5, 150 mM NaCl, 10% [wt/vol] glycerol, and 1% [wt/vol] Triton X-100), twice with 1 ml of buffer A (20 mM Tris-HCl, pH 7.5, 150 mM NaCl, and 1% [wt/vol] Triton X-100), and finally once with 1 ml of TNT buffer (50 mM Tris-HCl, pH 8.0, 150 mM NaCl, 1% [wt/vol] Triton X-100). The washed beads were incubated with 10 U of tobacco etch virus protease (Invitrogen) in TNT buffer (100 µl) to release bound protein complexes from the beads. After incubation for 60 min at room temperature, the supernatant was pooled and the beads were washed twice with 70 µl of buffer A. The resulting supernatants were combined and incubated with 12 µl of FLAG-Sepharose beads for the second immunoprecipitation. After incubation for 60 min at room temperature, the beads were washed three times with 240 µl of buffer A, and proteins bound to the immobilized HCV core protein on the FLAG beads were dissociated by incubation with 80 µg/ml FLAG peptide (NH_2-Asp-Tyr-Lys-Asp-Asp-Asp-Asp-Lys-COOH) (Sigma).

MS/MS. Proteins were separated by 9% sodium dodecyl sulfate-polyacrylamide gel electrophoresis (SDS-PAGE) and visualized by silver staining. The stained bands were excised and digested in the gel with lysylendoprotease-C (Lys-C), and the resulting peptide mixtures were analyzed using a direct nanoflow liquid chromatography-tandem mass spectrometry (MS/MS) system (33), equipped with an electrospray interface reversed-phase column, a nanoflow gradient device, a high-resolution Q-time of flight hybrid mass spectrometer (Q-TOF2; Micromass), and an automated data analysis system. All the MS/MS

spectra were searched against the nonredundant protein sequence database maintained at the National Center for Biotechnology Information using the Mascot program (Matrixscience) to identify proteins. The MS/MS signal assignments were also confirmed manually.

Expression and purification of recombinant proteins. *E. coli* BL21(DE3) cells were transformed with plasmids expressing GST fusion protein or His-tagged protein and grown at 37°C. Expression of the fusion protein was induced by 1 mM isopropyl-β-D-thiogalactopyranoside at 37°C for 4 h. Bacteria were harvested, suspended in lysis buffer (phosphate-buffered saline [PBS] containing 1% Triton X-100), and sonicated on ice.

Hi5 cells were infected with recombinant baculoviruses to produce GST-C173HT, GST-C152HT, GST-HT, MEF-E6AP, and His-tagged mouse E1 (17). GST and GST fusion proteins were purified on glutathione-Sepharose beads (Amersham Bioscience) according to the manufacturer's protocols. His-tagged proteins were purified on nickel-nitrilotriacetic acid beads (QIAGEN) according to the manufacturer's protocols. MEF-E6AP and MEF-E6AP C-A were purified on anti-FLAG M2 agarose beads (Sigma) according to the manufacturer's protocols.

Immunoblot analysis. Immunoblot analysis was performed essentially as described previously (11). The membrane was visualized with SuperSignal West Pico chemiluminescent substrate (Pierce).

HCV core protein and E6AP binding assays. To map the E6AP binding site on HCV core protein, 2.5 μg of purified recombinant GST-E6AP expressed in Hi5 cells was mixed with 1,000 μg of 293T cell lysates transfected with a series of FLAG-tagged HCV core deletion mutants as indicated. The protein concentration of the cells was determined using the bicinchoninic acid protein assay kit (Pierce). The mixtures were immunoprecipitated with anti-FLAG M2 agarose beads (Sigma), and proteins bound to the immobilized HCV core protein on anti-FLAG beads were dissociated with FLAG peptide (Sigma). The eluates were analyzed by immunoblotting with anti-GST PAb. To map the HCV core-binding site on E6AP, GST pull-down assays were performed as described previously (51).

In vivo ubiquitylation assay. In vivo ubiquitylation assays were performed essentially as described previously (57). FLAG-core was immunoprecipitated with anti-FLAG beads. Immunoprecipitates were analyzed by immunoblotting, using either anti-HA PAb or anticore PAb (TS1) to detect ubiquitylated core proteins.

In vitro ubiquitylation assay. For in vitro ubiquitylation of HCV core protein, purified GST-C173HT and GST-C152HT were used as substrates. Purified GST-HT was used as a negative control. Assays were done in 40-μl volumes containing 20 mM Tris-HCl, pH 7.6, 50 mM NaCl, 5 mM ATP, 10 mM MgCl$_2$, 8 μg of bovine ubiquitin (Sigma), 0.1 mM dithiothreitol, 200 ng mouse E1, 200 ng E2 (UbcH7), and 0.5 μg each of MEF-E6AP or MEF-E6AP C-A. The reaction mixtures were incubated at 37°C for 120 min followed by purification with glutathione-Sepharose beads and immunoblotting with the indicated antibodies.

siRNA transfection. 293T cells or Huh-7 cells at 3×10^5 cells in a six-well plate were transfected with 40 pmol of either E6AP-specific short interfering RNA (siRNA; Sigma) or scramble negative-control siRNA duplexes (Sigma) using HiPerFect transfection reagent (QIAGEN) following the manufacturer's instructions. The siRNA target sequences were as follows: E6AP (sense), 5′-GGGUC UACACCAGAUUGCUTT-3′; scramble negative control (sense), 5′-UUGCG GGUCUAAUCACCGATT-3′.

CHX half-life experiments. To examine the half-life of HCV core protein, transfected 293T cells were treated with 50 μg/ml cycloheximide (CHX) at 44 h posttransfection. The cells at zero time points were harvested immediately after treatment with CHX. Cells from subsequent time points were incubated in medium containing CHX at 37°C for 3, 6, and 9 h as indicated.

Infection of Huh-7 cells with secreted HCV. Infectious HCV JFH1 was produced in Huh-7.5.1 cells (61) as described previously (56). Culture supernatant containing infectious HCV JFH1 was collected and passed through a 0.22-μm filter. Naïve Huh-7 cells were seeded 24 h before infection at a density of 1×10^6 in a 10-cm dish. The cells were incubated with 2.5 ml of the inoculum (6.5×10^3 50% tissue culture infectious dose [TCID$_{50}$]/ml) for 3 h, washed three times with PBS, and supplemented with fresh complete Dulbecco's modified Eagle's medium. Then the cells were transfected with 6 μg each of pCAGGS, pCAG-HA-E6AP, or pCAG-HA-E6AP C-A by using TransIT LT1 (Mirus). The cells were trypsinized and replated in six-well plates at 1 day postinfection. The culture medium was changed every 2 days. The culture supernatants and the cells were collected at days 3 and 7 postinfection.

Quantitation of HCV RNA and core protein. We quantitated HCV core protein in cell lysate using the HCV core antigen enzyme-linked immunosorbent assay (ELISA) (Ortho-Clinical Diagnostics). Total RNA was extracted from cells

using TRIzol reagent (Invitrogen). To quantitate HCV RNAs, real-time reverse transcription-PCR was performed as described previously (53).

Infectivity assay. The TCID$_{50}$ was calculated essentially based on the method described previously (28). Virus titration was performed by seeding Huh-7 cells in 96-well plates at 1×10^4 cells/well. Samples were serially diluted fivefold in complete growth medium and used to infect the seeded cells (six wells per dilution). Following 3 days of incubation, the cells were immunostained for core with anticore MAb (2H9). Wells that expressed at least one core-expressing cell were counted as positive, and the TCID$_{50}$ was calculated.

Immunocytochemistry and fluorescence microscopy. Cells on collagen-coated coverslips were washed with PBS, fixed with 4% paraformaldehyde for 30 min at 4°C, and permeabilized with PBS containing 0.2% Triton X-100. Cells were preincubated with BlockAce (Dainippon Pharmaceuticals), incubated with specific antibodies as primary antibodies, washed, and incubated with rhodamine-conjugated goat anti-rabbit immunoglobulin G (ICN Pharmaceuticals, Inc.) and Qdot 565-conjugated goat anti-mouse immunoglobulin G (Quantumdot) as secondary antibody. Then the cells were washed with PBS, counterstained with DAPI (4′,6′-diamidino-2-phenylindole) solution (Sigma) for 3 min, mounted on glass slides, and examined with a BZ-8000 microscope (Keyence).

Knockdown of endogenous E6AP in HCV JFH1-infected Huh-7 cells. Naïve Huh-7 cells at 10^6 cells/10-cm dish were inoculated with 2.5 ml of the inoculum including infectious HCV JFH1 (6.5×10^3 TCID$_{50}$/ml) and cultured. The cells were replated in a six-well plate at 3×10^5 cells/well at day 11 postinfection and transfected with 40 pmol of E6AP siRNA or control siRNA. The culture medium was changed at 24 h after transfection. The cells were harvested at day 2 after transfection, and the intracellular core protein levels were quantitated using the HCV core antigen ELISA. The culture supernatants were collected at day 2 after transfection and assayed for TCID$_{50}$ determinations.

RESULTS

Identification of E6AP as an HCV core-binding protein. To identify the molecular machinery for HCV core ubiquitylation, we searched for endogenous ubiquitin-proteasome pathway proteins that associated with HCV core protein. HCV core-binding proteins (i.e., MEF core and its binding proteins, recovered from lysed cells) were purified by a tandem affinity purification procedure using a tandem tag (known as MEF tag) (16). Ten proteins were reproducibly detected (Fig. 1A, lane 2), but none were recovered from lysed control cells transfected with empty vector alone (Fig. 1A, lane 1).

To identify the proteins, silver-stained bands were excised from the gel, digested by Lys-C, and analyzed using a direct nanoflow liquid chromatography-MS/MS system. Nine proteins were identified: two known HCV core-binding proteins, human DEAD box protein DDX3 (38) and proteasome activator PA28γ (30), and seven potential HCV core-binding proteins. E6AP was identified (Fig. 1A, lane 2) on the basis of five independent MS/MS spectra (Table 1). Immunoblot analyses confirmed the proteomic identification of E6AP, DDX3, PA28γ, and MEF-core (Fig. 1B to E).

E6AP binding domain for HCV core protein. The E6AP binding domain for HCV core protein was investigated. Figure 2A is a schematic representation of E6AP and known motifs in E6AP. A series of deletion mutants of E6AP as GST fusion proteins were expressed in *E. coli*. GST pull-down assays found that the carboxyl-terminal deletion mutant E6AP (1–517), but not E6AP (1–418) (Fig. 2C, lanes C and D), and the amino-terminal deletion mutant E6AP (418–875), but not E6AP (517–875) (Fig. 2C, lanes J and K), were able to bind to the core protein. The signal was absent when unprogrammed wheat germ extracts (the negative control) were used as a source of proteins (data not shown). GST pull-down assays (Fig. 2B) found that the region from aa 418 to aa 517 is important for binding to the HCV core protein. An assay of the
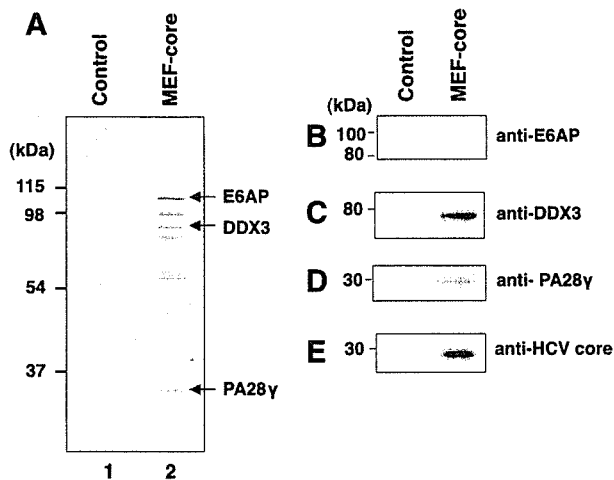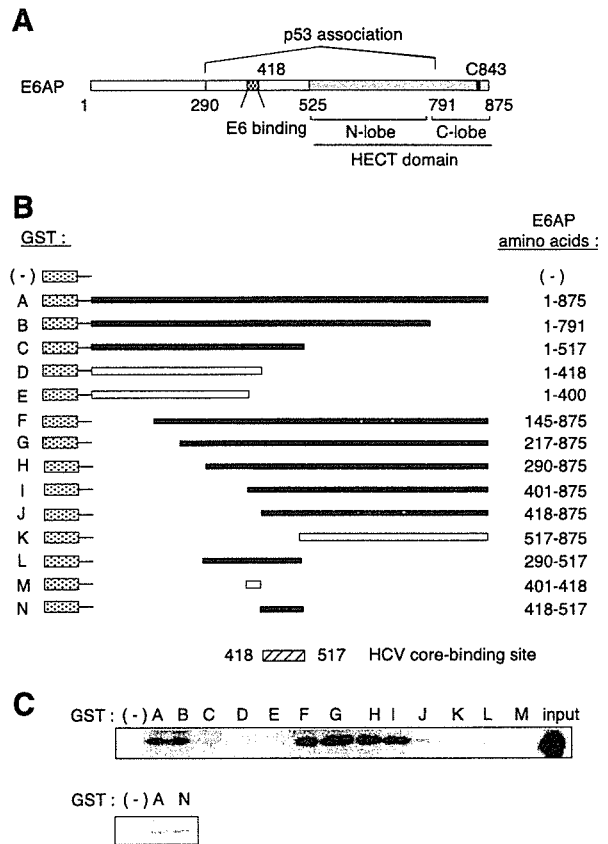
FIG. 1. HCV core protein associates with E6AP in vivo. (A) 293T cells were transfected with pcDNA3-MEF-core or empty plasmid, incubated for 48 h, and then harvested. The expressed MEF-core and binding proteins were recovered using the MEF purification procedure. Proteins bound to the MEF-core immobilized on anti-FLAG beads were dissociated with FLAG peptides, resolved by 9% SDS-PAGE, and visualized by silver staining. Control experiments were performed using 293T cells transfected with vector alone. The positions of E6AP, DDX3, and PA28γ are indicated by arrows. (B to E) The proteins detected in panel A were confirmed by immunoblotting with appropriate antibodies: E6AP (B), DDX3 (C), PA28γ (D), and MEF-core (E).

ability of GST-E6AP (418–517) to bind to the HCV core protein was confirmatory (Fig. 2C, lane N) and led to the conclusion that the HCV core-binding domain of E6AP was aa 418 to aa 517.

The HCV core-binding domain for E6AP. By use of a panel of HCV core deletion mutants (Fig. 3A), GST-E6AP was found to coimmunoprecipitate with all of the FLAG-core proteins (Fig. 3A, lanes A to H) except FLAG-core (72–191) or FLAG-core (92–191) (Fig. 3A, lanes I and J). No association of control GST protein with any FLAG-core proteins was observed (data not shown). These data suggest that the aa-58-to-aa-71 segment of the HCV core binds to E6AP. The ability of GST-core (58–71) to associate with purified MEF-E6AP confirmed that the core (aa 58–71) was the site for E6AP binding on the HCV core protein (Fig. 3B).

E6AP decreases steady-state levels of HCV core protein in 293T cells and HepG2 cells. One of the features of HECT domain ubiquitin ligases is direct association with their substrates (50). Thus, we hypothesized that E6AP would function as an E3 ubiquitin ligase for the HCV core protein. We as-

TABLE 1. Identification of E6AP by tandem mass spectrometry[a]

Peptide m/z	Sequence determined	Residues
720.9	VFSSAEALVQSFR	156–168
922.4	AACSAAAMEEDSEASSSR	196–213
774.9	MMETFQQLITYK	339–350
1,053.1	ITVLYSLVQGQQLNPYLR	507–524
809.4	EFVISYSDYILNK	712–724

[a] The protein was ubiquitin protein ligase E3A (E6AP) isoform 2 (GenBank accession no. NP_000453).

FIG. 2. Mapping of the HCV core-binding domain for E6AP. (A) Structure of E6AP. Shown is a schematic representation of the regions of E6AP isoform II that mediate E6 binding (aa 401 to 418), E6-dependent association with p53 (aa 290 to 791), and the HECT catalytic domain (aa 525 to 875). The catalytic cysteine residue is located at aa 843. (B) Schematic representation of GST-E6AP proteins. GST proteins A through N contain the E6AP amino acids indicated to the right. The shaded region of each represents the GST sequence. Closed boxes represent proteins that are bound specifically to HCV core protein, and open boxes represent those that are not bound. (C) Binding of HCV core protein to GST-E6AP proteins A through N. In vitro-translated core protein (aa 1 to 173) was assayed for association with GST (-) or the GST-E6AP fusion proteins A through N. Association of core protein was detected by immunoblotting with anti-core MAb.

sessed the effects of E6AP on the HCV core protein in 293T cells. FLAG-core (1–191) together with HA-tagged wild-type E6AP, catalytically inactive mutant E6AP, E6AP C-A (19), or WWP1 (another HECT domain ubiquitin ligase) (22) was introduced into 293T cells, and the levels of the core protein were examined by immunoblotting. The steady-state levels of the core protein decreased with an increase in the amount of E6AP plasmids (Fig. 4A and B). However, neither E6AP C-A mutant nor WWP1 decreased the steady-state levels of the core protein, suggesting that E6AP enhances degradation of the core protein.

To verify the critical need for endogenous E6AP in the core degradation, expression of E6AP was knocked down by siRNA and the expression of the core protein and E6AP was assayed by immunoblotting. Transfection of the E6AP-specific siRNA

A

HCV core
amino acids :

▨ FLAG-tag

HCV core

A. 1-191
B. 1-173
C. 1-152
D. 1-123
E. 1-111
F. 24-191
G. 38-191
H. 58-191
I. 72-191
J. 92-191

58 ☐ 71   E6AP-binding site

A B C D E F G H I J   input

GST-E6AP

FLAG-Core

A B C D E F G H I J

B

GST

GST-core (58-71)

CBB
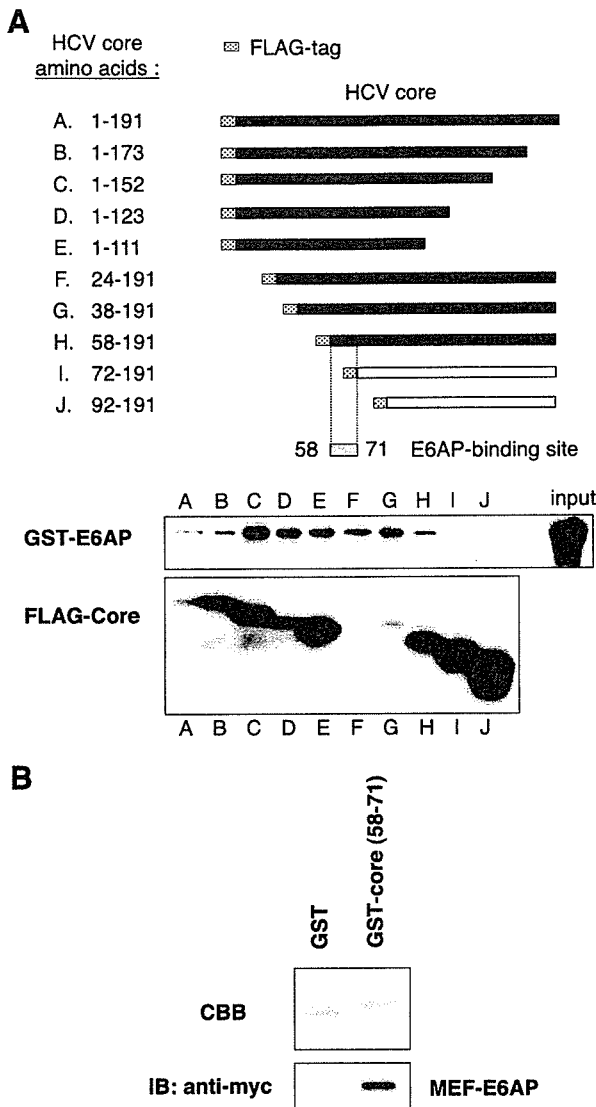
IB: anti-myc   MEF-E6AP

FIG. 3. Mapping of the E6AP binding domain for HCV core protein. (A) In vitro binding of E6AP to HCV core protein. 293T cells were transfected with each plasmid indicated in the upper panel. At 48 h posttransfection, cell lysates were mixed with purified GST-E6AP, immunoprecipitated with anti-FLAG beads, and then immunoblotted with anti-GST PAb (middle panel) or anti-FLAG MAb (bottom panel). The last lane (input) represents GST-E6AP used in this assay (middle panel). (B) Binding of GST-core (aa 58 to aa 71) to purified MEF-E6AP. GST served as a negative control for binding. Upper panel, Coomassie blue-stained SDS-PAGE of GST and GST-core (58–71). Lower panel, results of the GST pull-down assay. MEF-E6AP was detected by anti-myc MAb. CBB, Coomassie brilliant blue; IB, immunoblot.

duplex reduced the protein level of E6AP by 90% at 48 h posttransfection (Fig. 4C, middle panel). Immunoblotting revealed a 4.1-fold increase in the level of the core protein in the cells transfected with E6AP siRNA (Fig. 4C, top panel), suggesting that endogenous E6AP plays a role in the proteolysis of the HCV core protein.

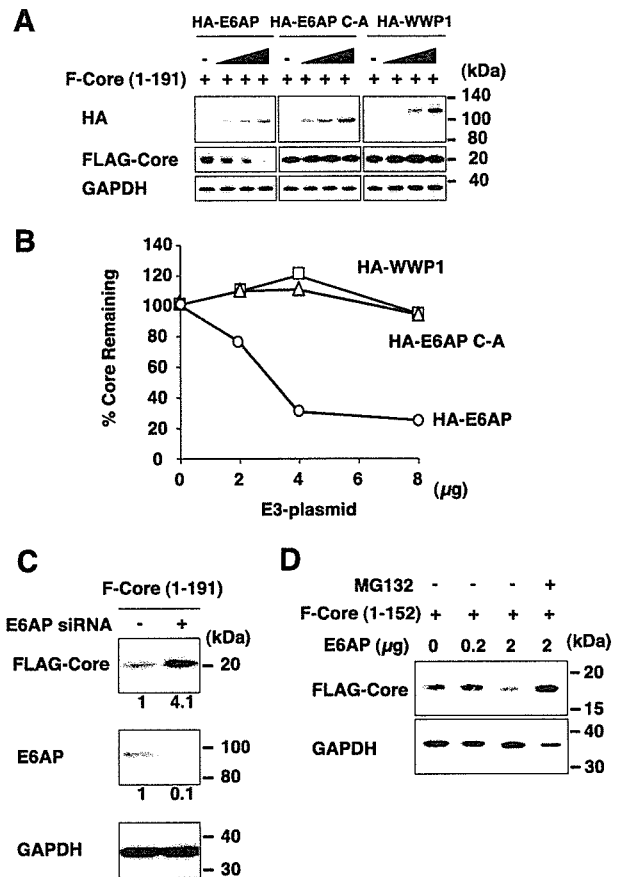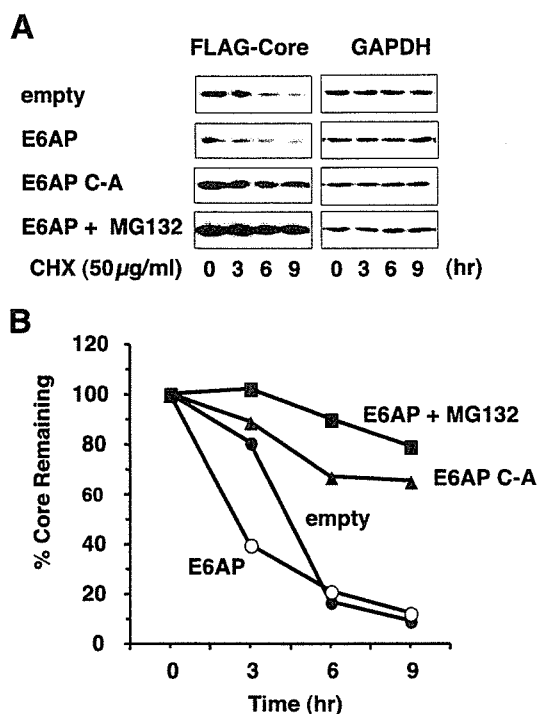Then we examined whether E6AP reduces the steady-state

A

HA-E6AP   HA-E6AP C-A   HA-WWP1

F-Core (1-191) + + + +   + + + +   + + + +   (kDa)

HA   — 140
                                            — 100
                                            — 80

FLAG-Core   — 20

GAPDH   — 40

B

FIG. 4. E6AP decreases steady-state levels of HCV core protein in 293T cells and in HepG2 cells. (A) 293T cells (1 × 10⁶ cells/10-cm dish) were transfected with 1 µg of pCAG FLAG-core (1–191) along with either pCAG-HA-E6AP, pCAG-HA-E6AP C-A, or pCAG-HA-WWP1 as indicated. At 48 h posttransfection, protein extracts were separated by SDS-PAGE and analyzed by immunoblotting with anti-HA PAb (top panel), anti-FLAG MAb (middle panel), and anti-GAPDH MAb (bottom panel). (B) Quantitation of data shown in panel A. Intensities of the gel bands were quantitated using the NIH Image 1.62 program. The level of GAPDH served as a loading control. Circles, E6AP; triangles, E6AP C-A; squares, WWP1. (C) Knockdown of endogenous E6AP by siRNA inhibits degradation of HCV core protein in 293T cells. 293T cells (3 × 10⁵ cells/six-well plate) were transfected with 40 pmol of E6AP-specific duplex siRNA (or control siRNA) as described in Materials and Methods. The cells were transfected with 2 µg of FLAG-core (1–191) expression plasmid and cultured for 24 h, harvested, and analyzed by immunoblotting. Shown is immunoblot detection of FLAG-tagged core protein (top panel), E6AP protein (middle panel), and GAPDH (bottom panel) in control siRNA-treated 293T cells or E6AP-siRNA-treated 293T cells. The relative levels of protein expression were quantitated by densitometry and indicated below in the respective lanes. GAPDH served as a loading control. (D) HepG2 cells (2 × 10⁵ cells/six-well plate) were transfected with pCAG FLAG-core (1–152) along with either empty vector or pCMV E6AP as indicated. The cells were harvested at 44 h posttransfection. Where indicated, cells were treated with 25 µM MG132 or with dimethyl sulfoxide control 14 h prior to collection. Equivalent amounts of the whole-cell lysates were separated by SDS-PAGE and analyzed by immunoblotting with anti-FLAG MAb (upper panel) or anti-GAPDH MAb (lower panel).
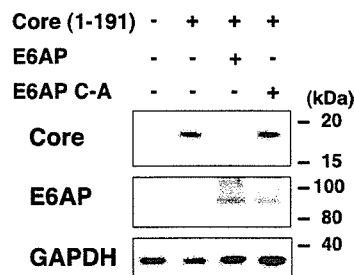
C

F-Core (1-191)

E6AP siRNA   -   +

FLAG-Core   (kDa)
                             — 20
             1   4.1

E6AP   — 100
                             — 80
             1   0.1

GAPDH   — 40
                             — 30

D

MG132   -   -   -   +
F-Core (1-152) +   +   +   +
E6AP (µg)   0   0.2   2   2   (kDa)

FLAG-Core   — 20
                              — 15

GAPDH   — 40
                              — 30

A

FLAG-Core   GAPDH

empty

E6AP

E6AP C-A

E6AP + MG132

CHX (50 μg/ml)   0 3 6 9   0 3 6 9   (hr)

B

FIG. 5. Kinetic analysis of E6AP-dependent degradation of HCV core protein. (A) 293T cells (1 × 10⁶ cells/10-cm dish) were transfected with 1 μg of pCAG-FLAG core (1–152) plus 4 μg of empty vector, pCMV-HA-E6AP, or pCMV-HA-E6AP C-A. The cells were treated with 50 μg/ml CHX at 44 h after transfection. Cell extracts were collected at 0, 3, 6, and 9 h after treatment with CHX, followed by immunoblotting. (B) Specific signals were quantitated by densitometry, and the percent remaining core at each time was compared with that at the starting point. The level of GAPDH served as a loading control. Open circles, E6AP; closed circles, empty plasmid; closed triangles, E6AP C-A; closed squares, E6AP with MG132 treatment. Data are representative of three independent experimental determinations.

levels of the core protein in hepatic cells as well as in 293T cells. Exogenous expression of E6AP resulted in reduction of the core protein in human hepatoblastoma HepG2 cells (Fig. 4D). Treatment of the cells with the proteasome inhibitor MG132 increased the core protein level, suggesting that the core protein was degraded through the ubiquitin-proteasome pathway. These results indicate that E6AP enhances proteasomal degradation of the HCV core protein in both hepatic cells and nonhepatic cells.

Kinetic analysis of E6AP-dependent degradation of HCV core protein. To determine whether the E6AP-induced reduction of the core protein is due to an increase in the rate of core degradation, we performed kinetic analysis using the protein synthesis inhibitor CHX. HCV core protein together with wild-type E6AP or inactive mutant E6AP C-A was expressed in 293T cells. At 44 h after transfection, cells were treated with either 50 μg/ml CHX alone or 50 μg/ml CHX plus 25 μM MG132 to inhibit proteasome function. Cells were collected at 0, 3, 6, and 9 h following treatment and analyzed by immunoblotting (Fig. 5A). Overexpression of E6AP resulted in rapid degradation of the core protein, whereas inactive mutant

Core (1-191) -   +   +   +

E6AP   -   -   +   -

E6AP C-A   -   -   -   +   (kDa)

Core   — 20
                                    — 15

E6AP   —100
                                    — 80

GAPDH   — 40

FIG. 6. E6AP promotes degradation of full-length HCV core protein in Huh-7 cells. Huh-7 cells (2 × 10⁵ cells/six-well plate) were transfected with 0.5 μg of pCAG-core (1–191) together with 2 μg of pCMV-HA-E6AP or pCMV-HA-E6AP C-A. At 48 h posttransfection, cells were harvested and analyzed by immunoblotting with anticore MAb (top panel), anti-E6AP PAb (middle panel), or anti-GAPDH MAb (bottom panel).

E6AP C-A increased the half-life of the core protein (Fig. 5B), suggesting that the inactive E6AP inhibited degradation of the core protein in a dominant-negative manner, which is in agreement with previous studies (19, 55). Treatment of the cells with MG132 inhibited the degradation of the core protein (Fig. 5B). Reverse transcription-PCR to determine mRNA levels of the HCV core gene and GAPDH gene found that neither wild-type E6AP nor inactive E6AP changed mRNA levels of the HCV core gene and GAPDH gene (data not shown). These results indicate that E6AP enhances proteasomal degradation of the core protein.

E6AP promotes degradation of the full-length core protein in Huh-7 cells. To determine whether the full-length HCV core protein expressed in hepatic cells is degraded through an E6AP-dependent pathway, human hepatoma Huh-7 cells were transfected with pCAG HCV core (1–191) along with either E6AP or E6AP C-A. To rule out the effects of N-terminal FLAG tag on the core degradation, HCV core protein was expressed as untagged protein. Expression of wild-type E6AP resulted in reduction of the core protein (Fig. 6). On the other hand, HCV core protein was not decreased after transfection of inactive E6AP, indicating that the full-length core protein expressed in Huh-7 cells is also degraded through an E6AP-dependent pathway.

E6AP mediates ubiquitylation of HCV core protein in vivo. To determine whether E6AP can induce ubiquitylation of HCV core protein in cells, we performed in vivo ubiquitylation assays. 293T cells were cotransfected with FLAG-core (1–191) and either E6AP or empty plasmid, together with a plasmid encoding HA-tagged ubiquitin to facilitate detection of ubiquitylated core protein. Cell lysates were immunoprecipitated with anti-FLAG MAb and immunoblotted with anti-HA PAb to detect ubiquitylated core protein (Fig. 7A). Only a little ubiquitin signal was observed on the core protein in the absence of cotransfected E6AP (Fig. 7A, lane 3). In contrast, coexpression of E6AP led to readily detectable ubiquitylated forms of the core protein as a ladder and a smear of higher-molecular-weight bands (Fig. 7A, compare lane 3 with lane 4). Immunoblot analysis with anticore PAb confirmed that FLAG-core proteins were immunoprecipitated (Fig. 7B, lanes 2 to 4, short exposure) and that higher-molecular-weight bands con-
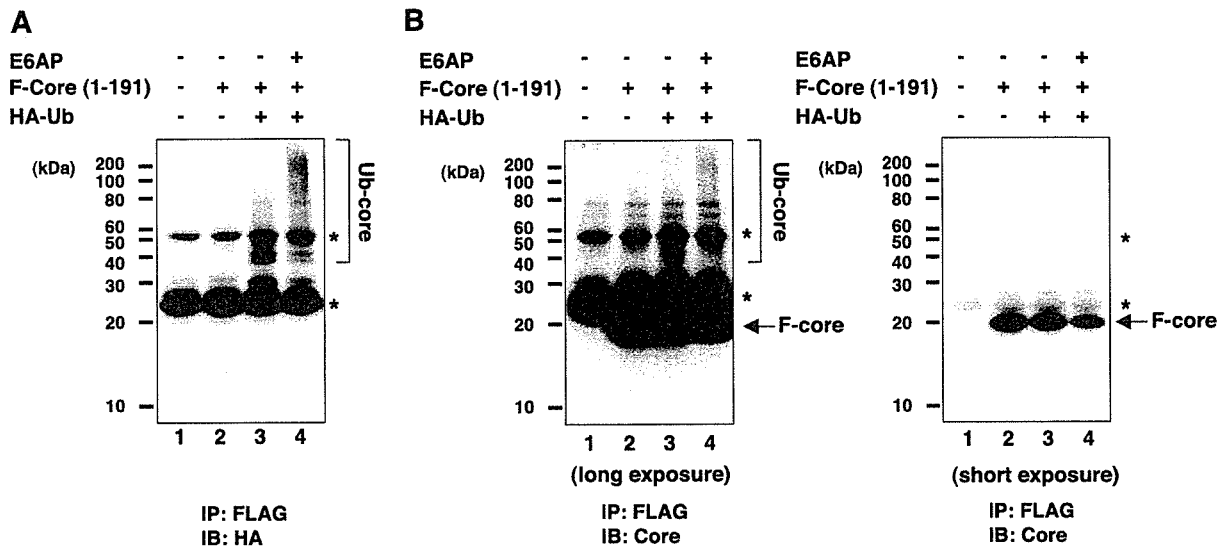
FIG. 7. E6AP-dependent ubiquitylation of HCV core protein in vivo. 293T cells (1 × 10^6 cells/10-cm dish) were transfected with 1 μg of pCAG FLAG-core (1–191) together with 2 μg of plasmid encoding E6AP as indicated. Each transfection also included 2 μg of plasmid encoding HA-ubiquitin. The cell lysates were immunoprecipitated with FLAG beads and analyzed by immunoblotting with anti-HA PAb (A) or anticore PAb (B). A shorter exposure of the core blot shows immunoprecipitated FLAG-core protein (B, right panel). A longer exposure of the core blot shows the presence of a ubiquitin smear (B, left panel). Asterisks indicate cross-reacting immunoglobulin light chain or heavy chain. Arrows indicate FLAG-core. IB, immunoblot; IP, immunoprecipitation.

jugated with HA-ubiquitin were indeed ubiquitylated forms of the core protein (Fig. 7B, lanes 3 and 4, long exposure).

E6AP mediates ubiquitylation of HCV core protein in vitro. To rule out the possibility that E6AP contributes to core protein degradation by inducing degradation of inhibitors of core turnover, we determined whether E6AP functions directly as a ubiquitin ligase by testing the ability of purified MEF-E6AP to mediate in vitro ubiquitylation of the purified recombinant HCV core protein. HCV core protein was expressed as a fusion protein containing N-terminal GST tag and C-terminal His tag and purified as described in Materials and Methods. GST-C173HT (aa 1–173) and GST-C152HT (aa 1–152) (see Materials and Methods) were used to determine whether the mature core protein and the C-terminally truncated core protein are targeted for ubiquitylation in vitro. The validity of this assay was established by demonstrating that E6AP but not E6AP C-A induced ATP-dependent ubiquitylation of GST-core protein. When in vitro ubiquitylation reactions were carried out either in the absence of MEF-E6AP or in the presence of MEF-E6AP C-A, no ubiquitylation signal was detected (Fig. 8A, lanes 4 and 5). However, inclusion of purified MEF-E6AP in the reaction mixture resulted in marked ubiquitylation of GST-C173HT (Fig. 8A, lane 6), while no ubiquitylation was observed in the absence of ATP (Fig. 8A, lane 7). No signal was detected when GST-HT was used as a substrate (Fig. 8A, lane 8). The higher-molecular-weight species of GST-core proteins were reactive with both anti-ubiquitin MAb (Fig. 8B, right panel, lanes 2 and 4) and anti-GST MAb (Fig. 8B, left panel, lanes 2 and 4). Both GST-C152HT and GST-C173HT were polyubiquitylated by E6AP in vitro (Fig. 8B), indicating that both the C-terminally truncated core and the mature core are polyubiquitylated by E6AP in vitro. These results revealed

that E6AP directly mediated ubiquitylation of HCV core proteins in an ATP-dependent manner.

Exogenous expression of E6AP reduces intracellular HCV core protein levels and supernatant infectivity titers in HCV-infected Huh-7 cells. We used a recently developed system for the production of infectious HCV particles using the HCV JFH1 strain (28, 56, 61) to examine whether E6AP can promote degradation of HCV core protein expressed from infectious HCV. E6AP-dependent core degradation was assessed in Huh-7 cells inoculated with the culture supernatant containing HCV JFH1. Levels of HCV core protein were detectable at day 3 postinfection and increased with time. Immunofluorescence staining for the core protein indicated that the percentage of HCV core-positive cells in the Huh-7 cells was almost 100 at day 7 postinfection. Transfection efficiency was 50 to 60% as measured with GFP-expressing plasmid. At day 7 postinfection, exogenous expression of E6AP reduced the intracellular core protein level by about 60% compared to the empty plasmid-transfected control cells (Fig. 9A). Inactive E6AP had little effect on the core protein levels. Total protein levels in the cells (Fig. 9B) and intracellular HCV RNA levels (Fig. 9C) did not change after transfection of wild-type E6AP or inactive E6AP. The immunofluorescence study revealed that HCV core protein was variably detected and the intensity of core staining was reduced in the cells staining positive for wild-type E6AP compared with neighboring cells staining negative for E6AP (Fig. 9E). Using inactive E6AP revealed colocalization of the core protein and E6AP in the perinuclear region (Fig. 9F) of HCV-infected cells. These results suggest that E6AP enhanced degradation of HCV core protein expressed from infectious HCV. Then we titrated HCV infectivity in the culture supernatant at day 7 postinfection by limiting
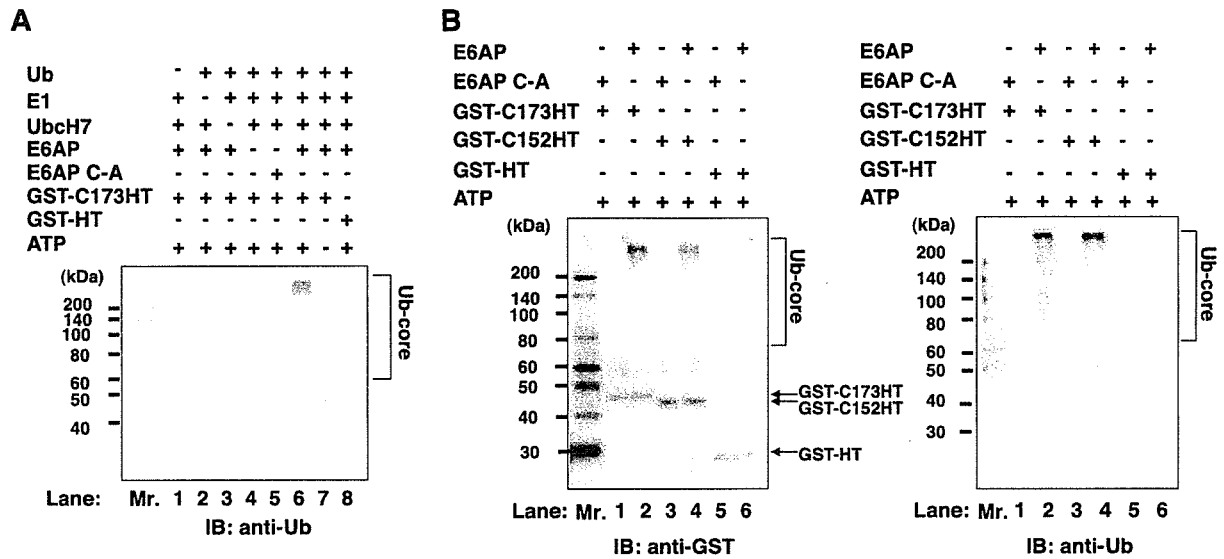
FIG. 8. In vitro ubiquitylation of HCV core protein by recombinant E6AP. For in vitro ubiquitylation of HCV core protein, purified GST-C173HT and GST-C152HT were used as substrates. Purified GST-HT was used as a negative control. Assays were done in 40-μl volumes containing each component as indicated. The reaction mixture is described in Materials and Methods. The reaction was carried out at 37°C for 120 min followed by purification with glutathione-Sepharose beads and analysis by immunoblotting with the indicated antibodies. Arrows indicate GST-C173HT, GST-C152HT, and GST-HT, respectively. Ubiquitylated species of GST-core proteins are marked by brackets. IB, immunoblot.

dilution assays. Exogenous expression of E6AP reduced the supernatant infectivity titer, whereas inactive E6AP had no effect on its infectivity titer (Fig. 9D), suggesting that the E6AP-dependent ubiquitin proteasome pathway affects the production of HCV particles through downregulation of the core protein.

E6AP silencing increases the levels of intracellular HCV core protein and supernatant infectivity titers in HCV-infected Huh-7 cells. Finally, to further validate the role of E6AP in HCV production, expression of endogenous E6AP was knocked down by siRNA and the HCV infectivity titers released from HCV JFH1-infected cells were examined. Knockdown of E6AP by siRNA led to an increase in intracellular core protein levels (Fig. 10A) and supernatant HCV infectivity titers (Fig. 10B). Taken together, our results suggest that E6AP mediates ubiquitylation and degradation of HCV core protein in HCV-infected cells, thereby affecting the production of HCV particles.

DISCUSSION

HCV core protein is a major component of viral nucleocapsid, plays a central role in viral assembly (25, 40), and contributes to viral pathogenesis and hepatocarcinogenesis (9). Therefore, it is important to clarify the molecular mechanisms that govern the cellular stability of this viral protein. We have previously reported that processing at the C-terminal hydrophobic domain of the core protein leads to efficient polyubiquitylation of the core protein (52). In this study, we identified E6AP as an HCV core-binding protein and showed that HCV core protein interacts with E6AP in vivo and in vitro, that E6AP enhances ubiquitylation and degradation of the mature core protein as well as the C-terminally truncated core protein, and that HCV core protein expressed from infectious HCV is

degraded via E6AP-dependent proteolysis. HCV core protein and E6AP were found to colocalize in the cytoplasm, especially in the perinuclear region. Moreover, exogenous expression of E6AP reduces intracellular core protein levels and supernatant HCV infectivity titers in HCV-infected Huh-7 cells. Knockdown of endogenous E6AP by siRNA increases intracellular core protein levels and supernatant infectivity titers in HCV-infected cells. These findings suggest that E6AP mediates ubiquitylation and degradation of HCV core protein, thereby affecting the production of HCV particles.

HCV core protein interacts with E6AP through the region of the core protein between aa 58 and aa 71. These 14 amino acids are highly conserved, with the first nine amino acids (PRGRRQPIP) present in the core protein of all the HCV genotypes (3). This result suggests that E6AP-dependent degradation of HCV core protein is common to all HCV genotypes and plays an important role in the HCV life cycle or viral pathogenesis. Our data indicated that HCV core proteins of genotypes 1b and 2a are subjected to proteolysis through an E6AP-mediated degradation pathway. We are currently examining whether E6AP promotes degradation of HCV core proteins of other genotypes.

Studies in addition to ours have reported that other HCV proteins, such as NS5B (8), the unglycosylated cytosolic form of E2 (39), NS2 (7), and F protein (58), are degraded through the ubiquitin-proteasome pathway. These studies suggest that the ubiquitin-proteasome pathway plays a role in the HCV life cycle or viral pathogenesis. To our knowledge, the present study is the first to demonstrate that the ubiquitin-proteasome pathway affects the HCV life cycle.

PA28γ was found to interact with HCV core protein in hepatocytes and promote proteasomal degradation of HCV core protein (30). PA28γ, however, has been shown to function
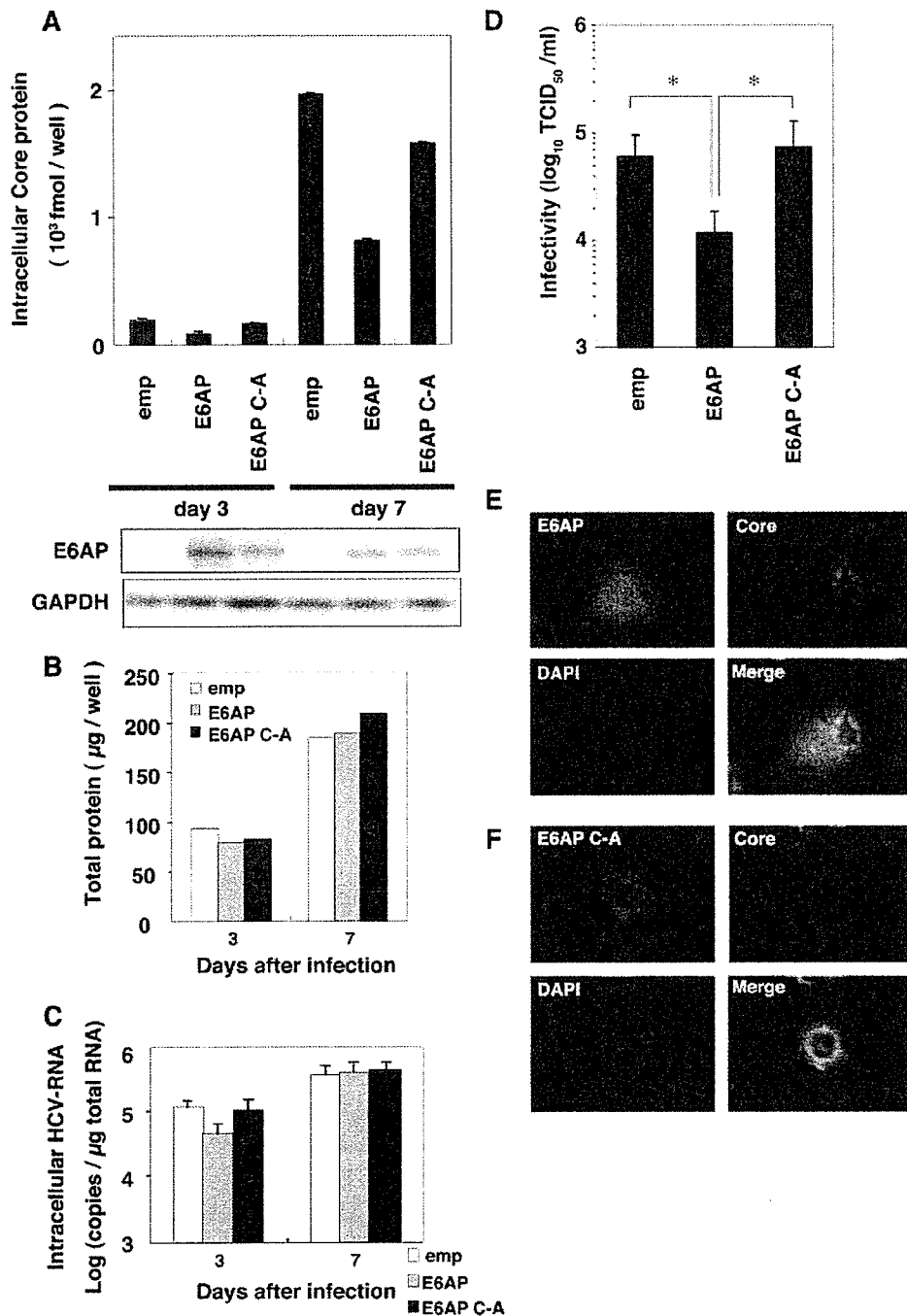
FIG. 9. Exogenous expression of E6AP reduces intracellular HCV core protein levels and supernatant infectivity titers in HCV-infected Huh-7 cells. Naïve Huh-7 cells were seeded as described in Materials and Methods; inoculated with 2.5 ml of the inoculum including infectious HCV JFH1 $(6.5 \times 10^3 \text{ TCID}_{50}/\text{ml})$; and transfected with 6 μg of empty plasmid, pCAG-HA-E6AP, or pCAG-HA-E6AP C-A. The culture supernatant and the cells were collected at days 3 and 7 postinfection. (A) Intracellular HCV core protein levels. (B) Levels of total protein. (C) Levels of intracellular HCV RNA in HCV-infected Huh-7 cells. Data represent the averages of three experiments with error bars. (D) Supernatant infectivity titers. At day 7 postinfection, culture supernatants were collected and assayed for TCID_{50} determinations. The difference between empty vector and E6AP or between E6AP and E6AP C-A was significant (*, $P < 0.05$, Student's t test). (E and F) HCV JFH1-infected Huh-7 cells were transfected with either MEF-E6AP plasmid or MEF-E6AP C-A plasmid, grown on coverslips, fixed, and processed for double-label immunofluorescence for HCV core and MEF-E6AP (E) or MEF-E6AP C-A (F). Anticore MAb (2H9) and anti-FLAG PAb were used as primary antibodies. Nuclei were visualized by staining the cells with DAPI. All the samples were examined with a BZ-8000 microscope. Representative images of individual cells are shown with merge images. emp, empty vector.
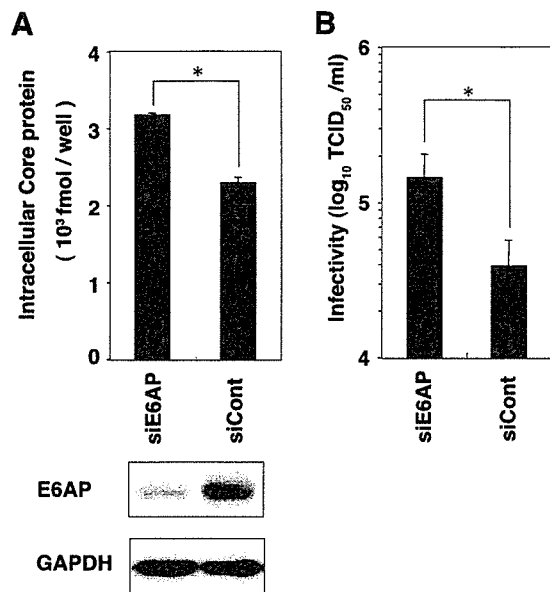
A

B

FIG. 10. E6AP silencing leads to an increase in the level of intracellular HCV core protein and supernatant infectivity titer in HCV-infected Huh-7 cells. (A) HCV JFH1-infected cells were replated in a six-well plate at 3×10^5 cells/well and transfected with 40 pmol of E6AP siRNA or control siRNA. The culture medium was changed at 24 h after transfection. The cells were harvested at day 2 after transfection, and the intracellular core protein levels were quantitated using the HCV core antigen ELISA. Equivalent amounts of the whole-cell lysates were separated by SDS-PAGE and analyzed by immunoblotting with anti-E6AP MAb or anti-GAPDH MAb. (B) Culture supernatants were collected at day 2 after transfection and assayed for $TCID_{50}$ determinations. For both panels, the difference between E6AP siRNA and control siRNA was significant (*, $P < 0.05$, Student's t test).

in a ubiquitin-independent, ATP-independent, and 20S proteasome-dependent pathway (27). There have been reports that several cellular factors, such as p53 (2), p73 (2), and RPN4 (18), are degraded through two alternative pathways, the ubiquitin-dependent 26S proteasome-dependent pathway and the ubiquitin-independent 20S proteasome-dependent pathway. Here we provide evidence that E6AP mediates ubiquitylation of HCV core protein. Still unclear is whether the PA28γ-dependent pathway requires polyubiquitylation of HCV core protein. HCV core protein is predominantly localized in the cytoplasm, especially at the endoplasmic reticulum membrane, on the surface of lipid droplets, and on mitochondria and mitochondrion-associated membranes (51). In HCV JFH1-infected cells, HCV core was found to localize in the cytoplasm and frequently to accumulate in the perinuclear region and the lipid droplets (44). Our results indicated that E6AP colocalized with HCV core protein especially in the perinuclear region. PA28γ was found to colocalize with HCV core protein in the nucleus. Functional differences may exist between the E6AP-dependent pathway and the PA28γ-dependent pathway in the stability control of HCV core protein. The functional role of the E6AP-dependent pathway and the PA28γ-dependent pathway remains to be elucidated.

The HCV core-binding region of E6AP was mapped to the region between aa 418 and aa 517. The multicopy maintenance protein 7, Mcm7, interacts with E6AP through a short motif,

termed the L2G box (aa 412 to 414), that lies within the E6 binding site of E6AP (23). Our data indicated that the E6 binding region containing the L2G motif is not required for interaction between HCV core protein and E6AP (Fig. 2C, lane M).

We propose here that E6AP may affect the production of HCV particles through controlling the amounts of HCV core protein. This mechanism may contribute to persistent infection. The E6AP binding domain of the core protein resides in the RNA-binding domain and binding domains for many host factors (40). These factors may affect the binding between E6AP and HCV core protein, resulting in control of E6AP-dependent core degradation. Another possibility is that HCV core protein may affect the normal function of E6AP, thereby contributing to pathogenesis. It will be intriguing to investigate whether HCV core protein has any effect on E6AP-dependent degradation of host factors. The other intriguing possibility is that HCV core-E6AP complex may function as an E3 ligase-like E6-E6AP complex to target host factors for proteasomal degradation and contribute to viral pathogenesis.

In conclusion, we have demonstrated that E6AP interacts with HCV core protein in vitro and in vivo and mediates ubiquitin-dependent degradation of the core protein, leading to downregulation of HCV particles. We propose that the E6AP-mediated ubiquitin-proteasome pathway may play a role in affecting the production of HCV particles through controlling the amounts of viral nucleocapsid protein. Identification of the specific E3 ubiquitin ligase may contribute to gaining a better understanding of the biology of the HCV life cycle as well as molecular details of the ubiquitin-dependent degradation of HCV core protein.

REFERENCES

1. Aizaki, H., Y. Aoki, T. Harada, K. Ishii, T. Suzuki, S. Nagamori, G. Toda, Y. Matsuura, and T. Miyamura. 1998. Full-length complementary DNA of hepatitis C virus genome from an infectious blood sample. Hepatology 27: 621–627.
2. Asher, G., P. Tsvetkov, C. Kahana, and Y. Shaul. 2005. A mechanism of ubiquitin-independent proteasomal degradation of the tumor suppressors p53 and p73. Genes Dev. 19:316–321.
3. Bukh, J., R. H. Purcell, and R. H. Miller. 1994. Sequence analysis of the core gene of 14 hepatitis C virus genotypes. Proc. Natl. Acad. Sci. USA 91:8239–8243.